



HAL
open science

Understanding sediment and carbon accumulation in macrotidal minerogenic saltmarshes for climate resilience

Benjamin Amann, Eric Chaumillon, Xavier Bertin, Cecilia Pignon-Mussaoud, Marie-Claire Perello, Christine Dupuy, Nathalie Long, Sabine Schmidt

► To cite this version:

Benjamin Amann, Eric Chaumillon, Xavier Bertin, Cecilia Pignon-Mussaoud, Marie-Claire Perello, et al.. Understanding sediment and carbon accumulation in macrotidal minerogenic saltmarshes for climate resilience. *Geomorphology*, 2024, 467, pp.109465. <https://doi.org/10.1016/j.geomorph.2024.109465> . hal-04747483v2

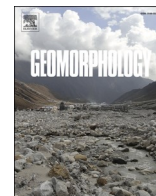
HAL Id: hal-04747483

<https://hal.science/hal-04747483v2>

Submitted on 12 Nov 2024

HAL is a multi-disciplinary open access archive for the deposit and dissemination of scientific research documents, whether they are published or not. The documents may come from teaching and research institutions in France or abroad, or from public or private research centers.

L'archive ouverte pluridisciplinaire **HAL**, est destinée au dépôt et à la diffusion de documents scientifiques de niveau recherche, publiés ou non, émanant des établissements d'enseignement et de recherche français ou étrangers, des laboratoires publics ou privés.



Understanding sediment and carbon accumulation in macrotidal minerogenic saltmarshes for climate resilience

Amann Benjamin^{a,*}, Chaumillon Eric^a, Bertin Xavier^a, Pignon-Mussaud Cécilia^a, Marie-Claire Perello^b, Christine Dupuy^a, Long Nathalie^a, Schmidt Sabine^b

^a Littoral ENvironnement et Sociétés (LIENSs), UMR 7266 CNRS, La Rochelle Université, 17000 La Rochelle, France

^b Univ. Bordeaux, CNRS, Bordeaux INP, EPOC, UMR 5805, F-33600 Pessac, France

ARTICLE INFO

Keywords:

Saltmarsh morphodynamics
Blue carbon
Sediment transport
Ecosystem services
Sea level rise
Coastal management

ABSTRACT

Coastal saltmarshes play an essential role in providing services such as sediment and carbon storage, coastal protection and support for biodiversity. Despite their importance, understanding the factors controlling sediment and carbon accumulation in these minerogenic saltmarshes remains challenging due to their diversity and site-specific characteristics. Understanding the respective role of these drivers is essential for effective coastal management, particularly for mitigating the impacts of climate change. This study evaluates the control of forcing factors on the lateral and vertical morphological evolution and carbon burial rates of three minerogenic saltmarshes located on the French Atlantic coast (Pertuis Charentais region). By focusing on these sites, the study isolates specific factors such as wind and wave exposure, inundation frequency, and sediment availability, while minimizing confounding influences like climate and tidal range. Results reveal significant lateral expansion of saltmarsh boundaries towards the sea across all sites, with the highest rates of progradation observed in the protected areas influenced by geomorphological features such as sand spits and sheltered bay heads. Sediment and mass accumulation rates (SAR; MAR), derived from ²¹⁰Pb and ¹³⁷Cs profiles of sediment cores ($n = 14$), range from 0.48 to 2.22 cm yr⁻¹, among the highest reported globally, with notable variability within and between sites. Inundation frequency and accommodation space explain SAR variability within sites, while sediment availability predominantly determines spatial differences in vertical accumulation rates between sites. Organic carbon burial rates range from 75 to 345 gC m⁻² yr⁻¹, and show a strong correlation with SAR ($r = 0.9$, $p < 0.001$, $n = 13$) but no dependence on carbon content or density ($r = 0.2$, $p > 0.05$, $n = 13$). This highlights the role of sediment input in the accumulation and sequestration of carbon by minerogenic saltmarshes. Furthermore, isotopic analysis indicates a marine source dominance in organic carbon sediment. This research provides insights into how different environmental conditions affect saltmarsh morphological evolution and carbon sequestration rates, informing targeted coastal management strategies focused on enhancing ecosystem resilience and climate resilience.

1. Introduction

The growing risk of marine submersions (IPCC, 2022) necessitates a reassessment of protective measures for coastal territories (Griggs and Reguero, 2021). A shift away from the exclusive reliance on heavy defences has been observed, with an increasing interest in the effectiveness of managed realignment as a means of addressing the evolving challenges of coastal hazards (Rupp-Armstrong and Nicholls, 2007; Huguet et al., 2018; Bongarts Lebbe et al., 2021). In this context, saltmarshes provide a number of important benefits. They are vegetated coastal

wetlands located in the upper tidal area that provide coastal protection, support for biodiversity, water quality and carbon burial and sequestration (Trumper et al., 2009; Leonardi et al., 2018; Bij de Vaate et al., 2020; Bertram et al., 2021). However, anticipating future alterations to these coastal wetlands and their impact on associated services remains inherently challenging, primarily due to gaps in our understanding of the site-specific functioning of these coastal environments (Pétillon et al., 2023). This has participated to limiting the number of existing managed realignment experiences globally (i.e., allowing coastal marsh areas previously protected from flooding to become flooded; Esteves,

* Corresponding author at: Littoral ENvironnement et Sociétés (LIENSs), UMR 7266 CNRS, La Rochelle Université, 17000 La Rochelle, France.

E-mail addresses: benjamin.amann@univ-lr.fr, benjamin.amann.france@gmail.com (A. Benjamin).

<https://doi.org/10.1016/j.geomorph.2024.109465>

Received 16 July 2024; Received in revised form 17 October 2024; Accepted 17 October 2024

Available online 23 October 2024

0169-555X/© 2024 The Authors. Published by Elsevier B.V. This is an open access article under the CC BY license (<http://creativecommons.org/licenses/by/4.0/>).

2014), with only a few instances in France (e.g., Adapto Program; www.lifeadapto.eu).

The provision of services by saltmarshes greatly depends on the morphological dynamics of these ecosystems (Wang et al., 2023). Saltmarshes are able to expand laterally and to elevate their topography in response to rising sea levels (Fagherazzi et al., 2020), especially minerogenic marshes fueled by sediments from inundating water (Van de Broek et al., 2018). With projected losses of saltmarshes due to sea-level rise globally, understanding the horizontal and vertical morphodynamics of these ecosystems is necessary for predicting their future trajectory, and ensuring the continuity of the services they provide (Schuerch et al., 2018).

The morphological dynamics of saltmarshes are influenced by various factors, which contribute to the complexity of the evolutions of these ecosystems (Townend et al., 2011; Yando et al., 2023). Global factors, such as climate conditions (Kirwan and Mudd, 2012; Ouyang and Lee, 2013) and sea-level changes (Schuerch et al., 2018; Rogers et al., 2019), are important drivers of the spatial variability in saltmarsh morphological evolution. Additionally, coastal factors such as tidal range (Kirwan and Guntenspergen, 2010), riverine input and sediment supply (Ladd et al., 2019; Baranes et al., 2022) and wind-wave action (Finotello et al., 2020; Mariotti and Fagherazzi, 2013; Tonelli et al., 2010) also play a significant role. Given the large number of forcing

parameters and the complexity of their interactions, it is challenging to discern the relative influence of each factor on saltmarsh morphological evolution. One approach to address this complexity is to compare saltmarshes within the same environment, thereby reducing the number of variables that may influence observed differences.

The present study was conducted on three saltmarshes located within the Pertuis Charentais region along the southern French Atlantic coast. The objective was to understand the influence of natural factors on the horizontal and vertical evolution of saltmarshes. This multi-site study, conducted in a region with a homogeneous climate, and comparable relative sea level rise ($2.8 \pm 0.7 \text{ mm yr}^{-1}$; www.sonel.org) and tidal range, allows for a detailed examination of the role of specific coastal factors including wind and wave exposure, inundation frequency, and sediment availability. Furthermore, the uniformity in vegetation composition across the three studied sites enabled an emphasis on physical processes rather than biological ones (e.g., biological productivity, competition, and community dynamics; Fagherazzi et al., 2005).

The morphological evolution of saltmarshes within and between the sites is discussed with respect to the controlling factors. Lateral changes are assessed by analysing shifts in saltmarsh boundaries through the use of aerial and satellite imagery. Sediment accumulation rates, indicative of vertical evolution, are determined through ^{210}Pb and ^{137}Cs profiles in sediment cores. The implications of these morphological changes are

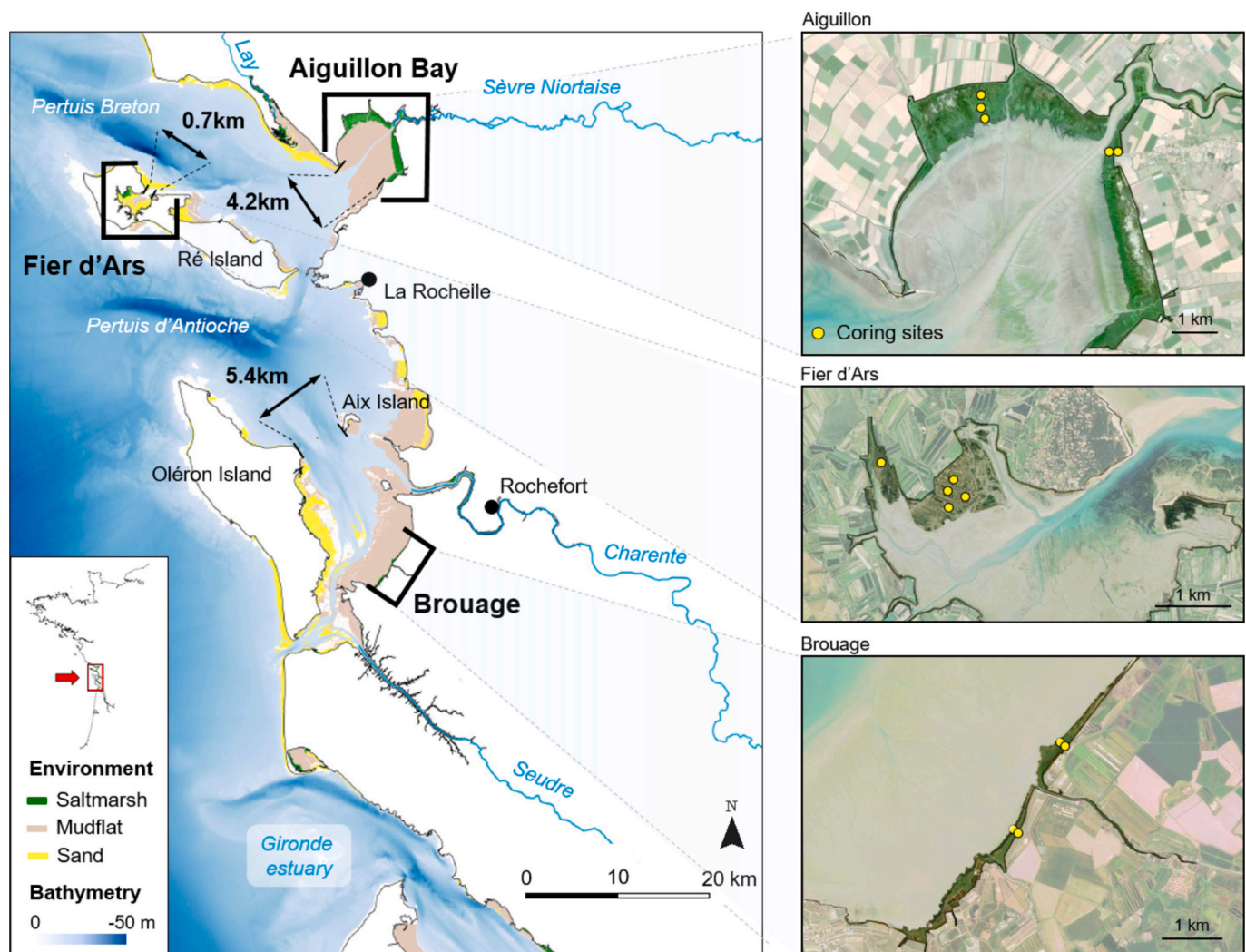


Fig. 1. Location of the three saltmarshes studied in the Pertuis Charentais Sea, SW France: Aiguillon, Fier d'Ars and Brouage; yellow dots on the images indicate coring sites. Data credits: coastal bathymetry from SHOM (<https://diffusion.shom.fr/donnees/bathymetrie/mnt-facade-atl-homonim.html>), coastal habitats from OFB/PNM EGMP (CARTHAM Project, 2012), images are ortho-imagery SPOT 6–7, 2023 (<https://openspot-dinamis.data-terra.org>).

then evaluated with regard to the carbon sink function of saltmarshes. This evaluation involves quantifying carbon burial rates, analysing the origin of organic carbon, and discussing the implications for coastal marsh management.

2. Studied sites

2.1. General settings

The three saltmarshes studied (Aiguillon, Brouage, Fier d'Ars) are located in the Pertuis Charentais Sea along the southwest coast of France (Fig. 1a). This region is characterized by a semidiurnal macrotidal regime, with a tidal range of up to 6.5 m (mean 3.8 m in La Rochelle Harbour; Dodet et al., 2019). The predominant wind direction is from the WSW to WNW (Bertin et al., 2015). These areas feature extensive sheltered mudflats (c. 3700 ha in Aiguillon Bay, 4000 ha in Brouage, and 500 ha in Fier d'Ars), with sediments composed mainly of clay/silt material (median grain size 8–17 μm ; Bocher et al., 2007). The halophytic vegetation of saltmarshes is dominated by C3 plants such as sea purslane (*Halimione portulacoides*) and marine puccinellia (*Puccinellia maritima*). Agropyron (*Agropyron pungentis*) are also observed in landward topographic high, while a few annual salicornia (*Salicornia europea*) compose lowland areas of the saltmarsh (Amann et al., 2023). C4 plants are mainly characterized by marine spartina (*Spartina maritima*) that develop principally in topographic low and at the mudflat/saltmarsh transition.

Four main rivers contribute to the input of freshwater and suspended sediments into the Pertuis Charentais Sea: the Lay (mean discharge 14.1 $\text{m}^3 \text{s}^{-1}$, in Bretonnière-la-Claye), the Sèvre Niortaise (20.1 $\text{m}^3 \text{s}^{-1}$, in Marans), the Charente (57.3 $\text{m}^3 \text{s}^{-1}$, in Saint-Savinien) and the Seudre (1.5 $\text{m}^3 \text{s}^{-1}$, in Corme-Ecluse) (www.hydro.eaufrance.fr). The influence of the Gironde Estuary on fine sediment supply has also been demonstrated in the southern area of the Pertuis Charentais (Constantin et al., 2018; Poirier et al., 2016; Fig. 1). With an estimated input to coastal waters of 1.6 Mt. yr^{-1} (Doxaran et al., 2009; Schmitt and Chaumillon, 2023), the Gironde estuary is also likely to contribute to the sediment budget of other areas within the Pertuis Charentais Sea. Mudflats are also important reservoirs of erodible fine-grained material for replenishing saltmarshes during periods of high tides and storms (Amann et al., 2023). Wind waves together with tidal currents promote mud resuspension and contribute to high suspended sediment concentrations in the shallow waters of the area (Bassoullet et al., 2000).

2.2. Saltmarsh morphology

All study sites are protected environments; however, they exhibit varying degrees of enclosure and exposure. The three sites, Aiguillon, Brouage and Fier d'Ars, show distinct geomorphological features and orientations, forming a gradient of wind-wave exposure from very protected to semi-exposed. Two of the sites, Aiguillon and Fier d'Ars, are semi-enclosed embayments, while the third site, Brouage, is an open coastal estuary.

Aiguillon Bay, a semi-enclosed embayment, is barred by the 'Pointe de l'Aiguillon' sand spit to the northwest with a bay mouth width of 4.2 km (Fig. 1). The intertidal area has a gentle slope (1.5 to 1.8/1000; Degré et al., 2006) with a gradual transition between the mudflat and pioneering saltmarsh vegetation. It hosts one of the largest saltmarshes in France, covering 1100 ha.

Fier d'Ars is another semi-enclosed embayment, enclosed by two sand spits, the 'Pointe du Fier' and the 'Pointe du Croc', with a bay opening width of 0.7 km (Fig. 1). The inlet between Fier d'Ars and the Pertuis Breton to the north is anchored by bedrock outcrops. Due to its northern location, the bay is protected from the strongest winds blowing from the south-west, west, and north-west. The saltmarshes of Fier d'Ars cover 65 ha and have developed since the end of the 19th century in sheltered tidal channels and former polders connected to the sea

(Lemesle et al., 2022).

The Brouage saltmarshes develop along a 5-km long estuarine open coast bordering the eastern side of the Marennes-Oléron Bay (Fig. 1). Although the Oléron Island protects Brouage from Atlantic swells (Bassoullet et al., 2000), northwestern winds can create a fetch of tens of kilometres generating wind waves with significant heights of up to 1 m at high tide in Brouage (Le Hir et al., 2010; Lavaud et al., 2020). These winds enter the Pertuis d'Antioche and reach the Brouage saltmarsh through the 5.4 km-wide bay mouth, between Oléron and Aix Island (Fig. 1). The saltmarsh platform is characterized locally by cliffs up to 1 m height at the transition with the mudflat, indicating susceptibility to sediment erosion by wave action (Koppel et al., 2005; Townend et al., 2011). Saltmarshes in Brouage cover 90 ha.

3. Materials and methods

3.1. Lateral evolution of the saltmarsh boundary

The position of the saltmarsh vegetation boundary for the years 1977, 2000, and 2020 was reconstructed using aerial photographs and satellite imagery, as described by Amann et al. (2023). The rate of saltmarsh boundary progression (in m yr^{-1}) was calculated from cross-shore transects using the USGS DSAS v5 tool (Himmelstoss et al., 2018). A positive rate indicates mean progradation over the studied period, while a negative rate indicates erosion.

3.2. Sampling and processing

Fourteen 1-m sediment cores were collected from saltmarshes at the three sites, in summer 2021 ($n_{\text{AIG}} = 5$; $n_{\text{BROU}} = 4$; $n_{\text{ARS}} = 5$; Fig. 1). Coring was done using a stainless steel Eijkkelkamp peat sampler. Its pivoting blade design helps minimize soil compression during sampling, thereby reducing potential bias in estimating sediment accretion rates. Cores were sliced every cm immediately on return to the laboratory and samples were weighed before and after being freeze-dried for 72 h to determine dry bulk density (DBD, in g cm^{-3}).

Surface vegetation representative of the main saltmarsh vegetation was collected, namely: *Halimione portulacoides*, *Puccinellia maritima*, *Agropyron pungentis*, *Salicornia europea* and *Spartina maritima*. Ten samples of each vegetation class were collected, rinsed, and freeze-dried before isotopic analysis. Below-ground biomass (BGB) was also separated from the bulk sediment in top cores and prepared for isotopic analysis following the same protocol as for the plant and bulk sediment samples.

3.3. Sediment and mass accumulation rates

The sediment and mass accumulation rates (SAR in cm yr^{-1} and MAR in $\text{g cm}^{-2} \text{yr}^{-1}$, respectively) were determined using ^{210}Pb excess ($^{210}\text{Pb}_{\text{xs}}$) profiles (Schmidt and Amann, 2024). ^{210}Pb ($t_{1/2} = 22.2 \text{ yr}$) is a naturally occurring radioisotope that is rapidly incorporated into sediments from atmospheric inputs. $^{210}\text{Pb}_{\text{xs}}$ decreases with sediment depth according its half-life and sedimentation rate. By applying this principle, SAR and MAR can be derived from $^{210}\text{Pb}_{\text{xs}}$ profile in sediment, based on the constant flux and constant sedimentation (CF:CS) method (Schmidt et al., 2014). The activities of ^{210}Pb , ^{226}Ra and ^{232}Th were measured in sediment samples using a BEGe™ Broad-Energy germanium detector (Mirion) equipped with a Cryocycle at EPOC, Bordeaux. Excesses of ^{210}Pb were calculated by subtracting the measured activity supported by its parent isotope, ^{226}Ra , from the total measured ^{210}Pb activity. To account for dilution due to the presence of vegetal fraction in the upper core sections, $^{210}\text{Pb}_{\text{xs}}$ activities were normalized to ^{232}Th (referred to as $^{210}\text{Pb}_{\text{xs}}^{\text{Th}}$, Amann et al., 2023). The coherence of sediment accumulation rates was independently tested using the time-stratigraphic marker ^{137}Cs . ^{137}Cs ($t_{1/2} = 30 \text{ yr}$) is an artificial radioisotope introduced by atmospheric nuclear tests, with maximum fallout

occurring in 1963.

3.4. Sediment grain size, carbon and nitrogen analysis

Sediment grain size was measured every three cm using a laser particle size analyzer at EPOC (Malvern Mastersizer 2000). Sample pre-treatments followed the methodology by Amann et al. (2023). Geometric mean grain size was obtained from three replicates, each measured for 12 s after 10 % sonication.

Soil organic carbon content (C_{org}), total nitrogen (TN), and $\delta^{13}C_{org}$ and $\delta^{15}N$ isotopes were determined c. every three cm of each core using an EA-IRMS in La Rochelle University, France (EA Isolink and Delta V Plus, Thermo Scientific). C_{org} and $\delta^{13}C_{org}$ were obtained from samples after acidification, while TN and $\delta^{15}N$ were measured on raw samples to prevent the effects of acidification (Lebreton et al., 2011). The ratio between C_{org} and TN (C/N) along with $\delta^{13}C$ and $\delta^{15}N$ were used to distinguish between autochthonous and allochthonous sources of organic matter. Surface vegetation ($n = 10$ for each of the four vegetation classes) and below-ground biomass were also analyzed by EA-IRMS following the sample protocol as for the bulk sediment samples.

Isotopic values were expressed in the δ unit notation as deviations from standards (Vienna Pee Dee Belemnite for $\delta^{13}C$ and atmospheric N_2 for $\delta^{15}N$) following the formula:

$$\delta^{13}C \text{ or } \delta^{15}N = \left(\frac{R_{sample}}{R_{standard}} - 1 \right) \cdot 10^3, \text{ where } R \text{ is } ^{13}C/^{12}C \text{ or } ^{15}N/^{14}N, \text{ respectively}$$

Reference materials USGS-61 and USGS-63 (Caffeine) were used for calibration and for uncertainty calculation. Standard deviations were 0.11 % for carbon, 0.10 % for nitrogen, and 0.05 ‰ for $\delta^{13}C$ and 0.04 ‰ for $\delta^{15}N$.

3.5. Organic carbon burial rates

Organic carbon burial rates (in $gC_{org} m^{-2} yr^{-1}$) were calculated as the product of the mean sediment C_{org} content (in %) and the $^{10}Pb_{xs}^{Th}$ derived MAR (in $g cm^{-2} yr^{-1}$). Only the sediment sections indicative of saltmarsh deposition in the cores were considered, extending until the depth marking the transition to underlying mudflat sediments. Surface layers were also excluded from the analysis to ensure that burial calculations were conducted below the zone of early diagenesis and intense organic matter degradation, thereby avoiding the overestimation of C_{org} stocks and burial rates due to highly-reactive carbon fractions (Williamson and Gattuso, 2022; Amann et al., 2023). The downcore profiles of C_{org} density reaching a stability were used as indication for effective preservation (Mueller et al., 2019; Amann et al., 2023).

3.6. Saltmarsh inundation frequency

The saltmarsh inundation frequency was estimated by intercepting the saltmarsh topography with a numerical water level hindcast performed from 1999 to 2022, as described in Lorrain-Soligon et al. (2023) and Savelli et al. (2019). This hindcast employs the circulation model SCHISM (Zhang et al., 2016), implemented in 2DH over the Pertuis Charentais Sea with a spatial resolution of 2000 m along the open boundary and 100 m close to the shoreline. SCHISM is forced by the amplitudes and phases of the 18 main tidal constituents linearly interpolated from the regional tidal model of (Bertin et al., 2012) and fields of sea-level pressure and 10 m winds originating from the CFSR reanalysis

(Saha et al., 2010). The model was run for the period 2000–2020 and hourly time series of water levels were extracted in front of each saltmarsh studied. The modeled water levels were compared with observations at several tide gauges in the area, showing a root mean squared discrepancy of 0.10 to 0.13 m (Lorrain-Soligon et al., 2023).

The derived recurrence curves in water surface elevation were subsequently compared with the topography of the saltmarshes, which was mapped using LiDAR-derived digital elevation models (DEMs; see Amann et al., 2023 for details on data accuracy). LiDAR data were acquired in 2021 by the departmental council of Charente maritime for Brouage and Fier d'Ars (© CD17 – MNT – 2021), and by the National Natural Reserve of the Aiguillon Bay for Aiguillon (© OPSIA Company, LIFE Program Aiguillon Bay 2016–2022).

3.7. Suspended sediment concentration in coastal waters

Suspended sediment concentrations (SSC, in $g m^{-3}$) in coastal waters near the three study sites were assessed using inorganic suspended particulate matter derived from ocean colour data for the period 2016–2021 (SPM-R: suspended matter regional algorithm, Aqua MODIS; Novoa et al., 2017). SPM-R data were accessed through the French marine data and service portal (ODATIS, <https://odatis.acri-st.fr>), which provides a 300-m spatial resolution mapping for the Pertuis Charentais.

SSC data were averaged from a 3-km cross-shore transect in front of each study site, providing representative averages and insights into spatial variations in sediment concentration.

4. Results

4.1. Lateral evolution of the saltmarshes

The reconstruction of saltmarsh vegetation boundaries between 1977, 2000, and 2020 reveals differences in lateral morphological evolutions among the three study sites (Fig. 2).

In the Fier d'Ars, saltmarshes show lateral evolution rates ranging from $+0.5$ to $+8.2 m yr^{-1}$, with an average progradation rate of $+3 m yr^{-1}$ over the period 1977–2020. The most rapid vegetation development occurs in the sheltered bay heads, while the slowest is observed in the historical polders located in the northern area (Fig. 2a). Aiguillon Bay exhibits the most rapid development of saltmarsh vegetation, ranging from $+0.8$ to $+14 m yr^{-1}$, with a mean seaward migration of $+8 m yr^{-1}$. The highest rates are observed in the northern sheltered bay, while the lowest rates are found near the river mouth separating the northern and southern parts of the bay (Fig. 2b). The Brouage saltmarshes is characterized by the lowest evolution rates of the three sites, ranging from -1.2 to $+3.3 m yr^{-1}$, with an average of $+0.7 m yr^{-1}$. The southern saltmarshes have higher rates, contrasting with the erosive northern sections. Maximum erosion occurs at the vegetation tip near the mouth of the inlet separating the two saltmarshes (Fig. 2c).

4.2. Sediment composition

The saltmarsh sediments are mainly composed of fine silt ($81 \pm 5 \%$) and clay ($17 \pm 5 \%$), with a mean grain size of $7 \pm 2 \mu m$. This grain size composition is consistent across the study sites, except for sediment cores collected within the historic polders in the Fier d'Ars (ARS-01 to -03). These cores reveal a sandy substratum below the saltmarsh, with a

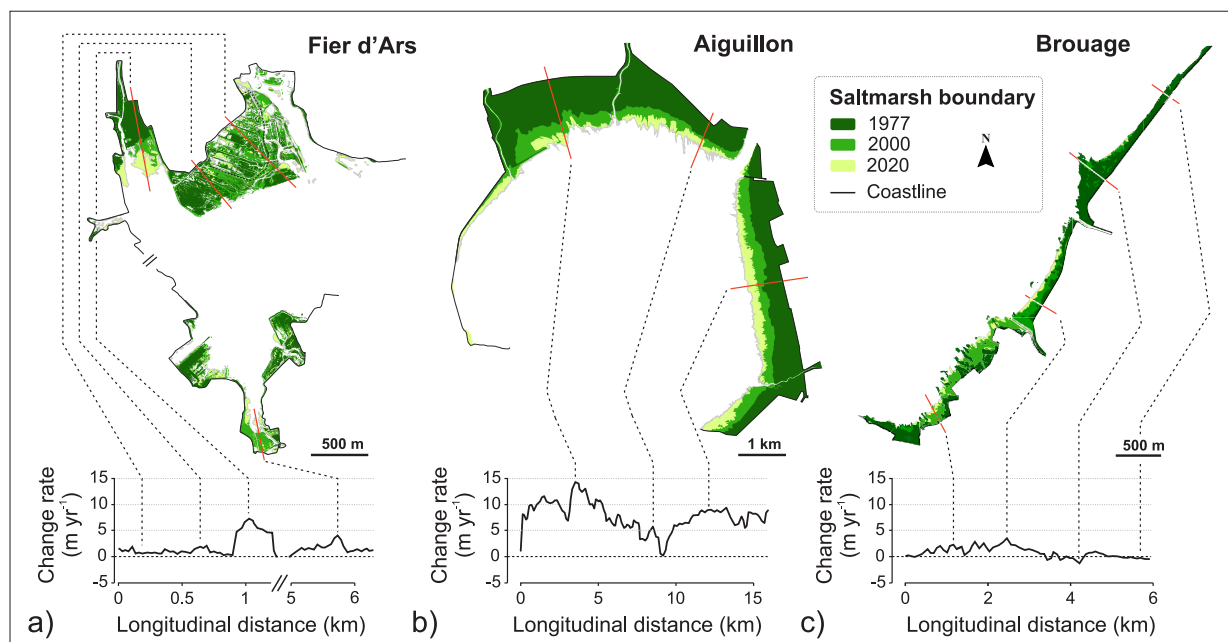


Fig. 2. Lateral evolution of the saltmarsh boundary and area reconstructed over three years: 1977, 2000, 2020 for a) Fier d'Ars, b) Aiguillon, and c) Brouage. Mean rates of change (lower panel, in m yr^{-1}) were calculated along longitudinal transects in each site for the cumulative period 1977–2020. Specific examples are indicated along selected transects (red lines traversing the saltmarshes).

clear transition from sand-dominated bottom to silt-dominated sediments at top (transition depth at 33 cm in ARS-01, 29 cm in ARS-02, and 57 cm in ARS-03). Only the muddy sediment section above this sandy substratum was included in the calculation of sediment and carbon accumulation rates in Fier d'Ars. Accordingly, dry bulk density (DBD) shows similar values among the cores and studied sites, averaging $0.8 \pm 0.1 \text{ g cm}^{-3}$ in Aiguillon, $0.9 \pm 0.1 \text{ g cm}^{-3}$ in Brouage, and $0.8 \pm 0.1 \text{ g cm}^{-3}$ in Fier d'Ars, despite variations in core length.

4.3. Vertical evolution of the saltmarshes

4.3.1. Sediment and mass accumulation rates

The activities of $^{210}\text{Pb}_{\text{xs}}$ are between 80 and 110 mBq g^{-1} in surface sediment and exhibit an exponential decrease with increasing depth beyond a potential mixed layer. The threshold of 10 mBq g^{-1} is reached at depths from approximately 30 cm to >110 cm, indicating significant differences in sediment accumulation rates across the different coring sites.

The mean sediment accumulation rates (SAR) and mass accumulation rates (MAR), calculated from $^{210}\text{Pb}_{\text{xs}}^{\text{Th}}$, range from 0.48 to 2.22 cm yr^{-1} and from 0.42 to 1.83 $\text{g cm}^{-2} \text{ yr}^{-1}$, respectively (Table 1). These rates are supported by the ^{137}Cs profiles, which exhibit a peak in ^{137}Cs at the expected depth based on the ^{210}Pb -MAR (Fig. 3). However, this is not the case for cores that are too short (AIG21_11, AIG17_01), particularly when the MAR is high (AIG21_20). Also, cores from historical polders in Fier d'Ars (ARS21_01, ARS21_02, ARS21_03) do not allow to detect ^{137}Cs peaks in the underlying sand layers.

SAR and MAR vary within and among the three studied saltmarshes, highlighting significant spatial differences in sediment dynamics.

4.3.2. Intra-site variability

SARs along cross-shore transects in the Aiguillon Bay and Brouage saltmarshes show an upward trend from landward to seaward stations (Fig. 3a, c). In Aiguillon Bay, SAR values are lowest at the landward station (0.84 cm yr^{-1}), increasing at the middle (1.85 cm yr^{-1}) and seaward stations (2.22 cm yr^{-1}). Similarly, the lowest values in Brouage are found at the two landward locations (1.11 cm yr^{-1} and 1.79 cm yr^{-1}), increasing seaward (1.85 cm yr^{-1} and 1.83 cm yr^{-1} , respective to

the two transects).

In the Fier d'Ars, the lowest SARs are observed in saltmarshes that developed on former polders (0.48 cm yr^{-1} and 0.49 cm yr^{-1}), with one exception showing a relatively high value (0.80 cm yr^{-1} ; Fig. 3b). The highest values are found outside these historical polders with no significant variability between the coring sites (0.84 cm yr^{-1} and 0.82 cm yr^{-1} , respectively).

4.3.3. Inter-site variability

SARs reveal significant differences between the three sites (Fig. 3). The Fier d'Ars saltmarshes show the lowest mean SAR with 0.69 cm yr^{-1} (0.48–0.84 cm yr^{-1}), which differs significantly ($p < 0.01$) from those of Brouage with 1.64 cm yr^{-1} (1.11–1.85 cm yr^{-1}), and Aiguillon with 1.51 cm yr^{-1} (0.84–2.22 cm yr^{-1}). The SAR values are not statistically different ($p > 0.05$) between Aiguillon and Brouage.

4.4. Organic carbon density, content and burial rates

C_{org} density profiles show a range between 0.01 and 0.03 g cm^{-3} (equivalent 1.3 to 6.2 % C_{org}) with the highest values found in the uppermost sections of the cores, indicative of a greater contribution of marsh vegetation to the carbon stocks (Fig. 4). C_{org} density decreases gradually with depth and remains constant below 20-cm depth, regardless of the core or site considered. This stability reached downcore by C_{org} density correspond to mean C_{org} values of $1.9 \pm 0.4 \%$ in Aiguillon, $1.5 \pm 0.1 \%$ in Brouage, and $1.8 \pm 0.5 \%$ in Fier d'Ars (Table 1).

C_{org} burial rates vary between 75 and 345 $\text{gC m}^{-2} \text{ yr}^{-1}$ among the three sites, and show a clear correlation with SAR variability ($r = 0.9$, $p < 0.001$, $n = 13$), but no significant dependence on C_{org} content or density ($r = 0.2$, $p > 0.05$, $n = 13$). Consequently, C_{org} burial rates are the lowest in the Fier d'Ars averaging $92 \pm 11 \text{ gC m}^{-2} \text{ yr}^{-1}$, whereas significantly ($p < 0.01$) higher burial rates are observed in Aiguillon and Brouage, with averages of 241 $\pm 118 \text{ gC m}^{-2} \text{ yr}^{-1}$ and 211 $\pm 46 \text{ gC m}^{-2} \text{ yr}^{-1}$, respectively (Table 1).

Table 1

Data synthesis for the saltmarshes in Aiguillon, Brouage, and Fier d'Ars, including sediment accumulation rates (SAR in cm yr^{-1}), mass accumulation rates (MAR, in $\text{g m}^{-2} \text{yr}^{-1}$), C_{org} content (in %), C_{org} burial rates (in $\text{gC m}^{-2} \text{yr}^{-1}$), and carbon sequestration capacity (converted in $\text{TCO}_{2\text{eq}} \text{ha}^{-1} \text{yr}^{-1}$). A mean value is given for each saltmarsh site and a weighted average is given for carbon burial and sequestration rates for the Pertuis Charentais accounting for the saltmarsh area in each site, i.e., 1100 ha in Aiguillon (88 % weight), 90 ha in Brouage (7 % weight), 65 ha in Fier d'Ars (5 % weight). See Fig. 3 for coring site locations. *SAR and MAR are based on $^{210}\text{Pb}_{\text{xs}}$, without Th standardizing.

Site	Coring site	Coordinates		SAR (cm yr^{-1})	MAR ($\text{g cm}^{-2} \text{yr}^{-1}$)	C_{org} content (%)	C_{org} burial rate ($\text{g m}^{-2} \text{yr}^{-1}$)	C sequestration rate ($\text{TCO}_{2\text{eq}} \text{ha}^{-1} \text{yr}^{-1}$)
		Latitude N	Longitude E					
Aiguillon	Northern transect							
	AIG21_20	46.3111	-1.1744	2.22 ± 0.32	1.83 ± 0.30	1.81 ± 0.34	331 ± 54	12.1 ± 2
	AIG21_21	46.3129	-1.1762	1.85 ± 0.09	1.50 ± 0.07	2.30 ± 0.09	345 ± 16	12.7 ± 0.6
	AIG21_22	46.3159	-1.1759	0.84 ± 0.06	0.74 ± 0.05	1.34 ± 0.13	99 ± 7	3.6 ± 0.3
	Eastern transect							
	AIG17_01	46.3032	-1.1313	$1.41 \pm 0.19^*$	$1.24 \pm 0.20^*$	-	-	-
	AIG21_11	46.3025	-1.1291	1.24 ± 0.26	0.86 ± 0.12	2.17 ± 0.58	187 ± 26	6.9 ± 1.0
	Mean value			1.51 ± 0.54	1.23 ± 0.45	1.9 ± 0.43	241 ± 118	8.8 ± 4.3
Brouage	Northern transect							
	BROU21_20	45.8856	-1.0964	1.85 ± 0.21	1.64 ± 0.16	1.52 ± 0.30	249 ± 24	9.1 ± 0.9
	BROU21_21	45.8853	-1.0959	1.11 ± 0.08	1.00 ± 0.07	1.45 ± 0.40	145 ± 10	5.3 ± 0.4
	Southern transect							
	BROU21_10	45.8722	-1.1053	1.83 ± 0.11	1.56 ± 0.12	1.50 ± 0.17	234 ± 18	8.6 ± 0.7
	BROU21_11	45.8720	-1.1048	1.79 ± 0.08	1.66 ± 0.13	1.30 ± 0.15	211 ± 17	7.7 ± 0.6
	Mean value			1.64 ± 0.36	1.46 ± 0.31	1.46 ± 0.11	211 ± 46	7.7 ± 1.7
Fier d'Ars	RNN Lilleau des Niges							
	ARS21_01	46.2287	-1.5029	0.48 ± 0.03	0.42 ± 0.04	1.78 ± 0.19	75 ± 7	2.8 ± 0.3
	ARS21_02	46.2280	-1.4990	0.49 ± 0.09	0.34 ± 0.06	2.71 ± 0.28	92 ± 16	3.4 ± 0.6
	ARS21_03	46.2294	-1.5027	0.80 ± 0.05	0.74 ± 0.05	1.41 ± 0.26	104 ± 7	3.8 ± 0.3
	ARS21_04	46.2268	-1.5039	0.82 ± 0.08	0.63 ± 0.08	1.46 ± 0.27	92 ± 12	3.4 ± 0.4
	Sheltered bay head							
ARS21_05	46.2309	-1.5125	0.84 ± 0.08	0.60 ± 0.06	1.63 ± 0.35	98 ± 10	3.6 ± 0.4	
	Mean value			0.69 ± 0.18	0.55 ± 0.15	1.80 ± 0.53	92 ± 11	3.4 ± 0.4
Pertuis Charentais	Weighed average			-	-	-	$231 \pm 108 \text{ gC m}^{-2} \text{yr}^{-1}$	$8.4 \pm 3.9 \text{ TCO}_{2\text{eq}} \text{ha}^{-1} \text{yr}^{-1}$

4.5. Isotopic signature of sediment organic carbon

The results from carbon isotopes ($\delta^{13}\text{C}$) are presented in relation to the carbon-to-nitrogen ratio (C/N), indicative of the origin of C_{org} in saltmarsh sediments; i.e., an autochthonous vs allochthonous source (Table 1, Fig. 5). The $\delta^{13}\text{C}$ and C/N values of the surface cores generally reflect the signature of saltmarsh terrestrial plants, such as *C3 Halimione p.*, *Agropyron p.*, and *Puccinellia m.*, and *C4 Spartina m.* (Fig. 5, Table 2). With increasing sediment depth, the C/N ratio gradually decreases across all cores, while the $\delta^{13}\text{C}$ values converge towards -22 ‰ , indicative of the allochthonous marine signature of C_{org} (marine POC: $\delta^{13}\text{C} = -25.1$ to -20.9 ‰ ; C/N = 4.2 to 7.7; SOMLIT station; www.somlit.fr). Basal-core sediments correspond to mudflat sediments ($\delta^{13}\text{C} = -22.0 \pm 0.2 \text{ ‰}$; C/N = 6.7 ± 0.5). This observed pattern has been discussed in detail for the Aiguillon Bay by Amann et al. (2023).

4.6. Topography, inundation frequency and SSC

4.6.1. Topography and inundation frequency

The topography of the saltmarsh platforms varies between the three

sites studied (Fig. 6). The Aiguillon and Brouage saltmarshes exhibit the highest mean elevations ($2.7 \pm 0.1 \text{ mNGF}$ and $3.0 \pm 0.2 \text{ mNGF}$, respectively), whereas the topography in the Fier d'Ars is significantly lower ($2.2 \pm 0.2 \text{ mNGF}$).

Despite the fact that the Fier d'Ars has the lowest water level recurrence curve, the saltmarshes in this area are more frequently flooded ($p < 0.01$), with a mean inundation frequency of $5.4 \pm 2.5 \text{ ‰}$ compared to $1.4 \pm 1.2 \text{ ‰}$ in Aiguillon and $0.6 \pm 2.1 \text{ ‰}$ in Brouage.

4.6.2. Suspended sediment concentrations (SSC)

Coastal water SSC for the period 2016–2021 provides an insight into the sediment availability for the three saltmarshes (Fig. 7). The highest SSC is found seaward of Brouage ($29.8 \pm 5.8 \text{ g m}^{-3}$) and Aiguillon ($23.7 \pm 6.8 \text{ g m}^{-3}$), while Fier d'Ars exhibits a significantly lower ($p < 0.01$) mean value ($7.5 \pm 3.3 \text{ g m}^{-3}$).

5. Discussion

5.1. Controls on lateral progradation

The lateral evolution of saltmarsh vegetation exhibited significant progradation trends towards the ocean in all study sites in the Pertuis Charentais region (Fig. 2). The highest rates of vegetation expansion were observed in sheltered areas, such as the northern Aiguillon Bay, which is shielded by a sand spit, and in sheltered bay heads of the Fier

d'Ars. Conversely, the slowest mean progradation rates occurred in Brouage, with some areas experiencing erosion. Exposure to wave and wind action, combined with the open-coast morphology of the estuary, likely limits vegetation growth in Brouage. Wind waves, especially wave power density, can control the lateral retreat of saltmarsh margins as attested by cliffs and overwash deposits (Marani et al., 2011; Finotello et al., 2020). The mudflat facing Brouage saltmarsh has a lower topography compared to the Aiguillon saltmarsh (approximately 0.7 m lower; Fig. 5), which further enhances its vulnerability to erosion by waves.

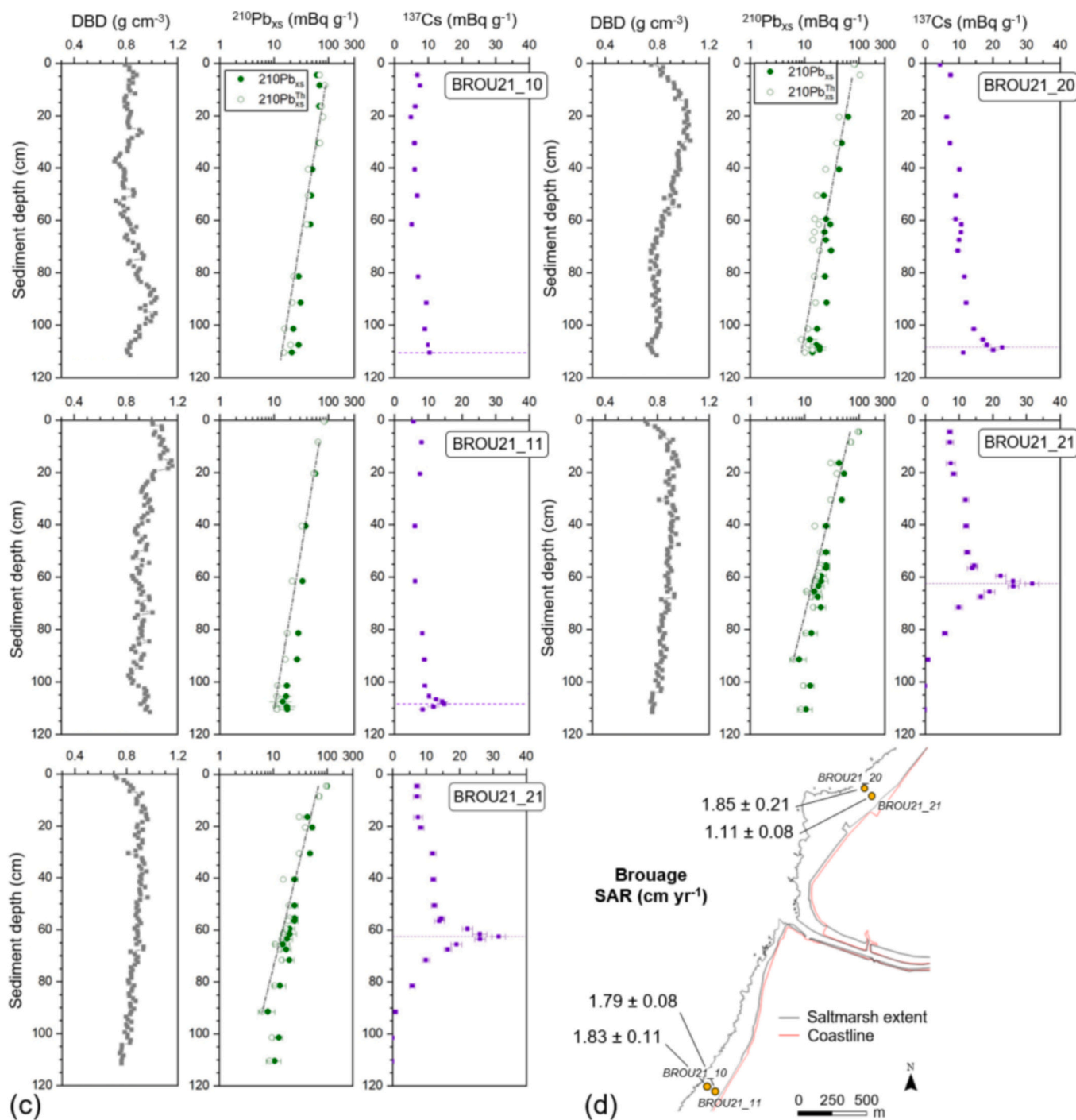


Fig. 3. Profiles with sediment depth of dry bulk density (DBD; gray), $^{210}\text{Pb}_{\text{xs}}$ and $^{210}\text{Pb}_{\text{xsTh}}$ (filled and empty green circles, respectively), and ^{137}Cs (purple), and the spatial variability in sediment accumulation rates (SAR, in cm yr^{-1}) obtained using ^{210}Pb and ^{137}Cs profiles from sediment cores for (a, b) Brouage, and (c, d) Fier d'Ars. Data from Aiguillon saltmarshes can be found in Table 1 (Amann et al., 2023). The gray horizontal rectangular cores shows the presence of sand. The purple horizontal dash line is the expected depth of ^{137}Cs peak considering ^{210}Pb -MAR.

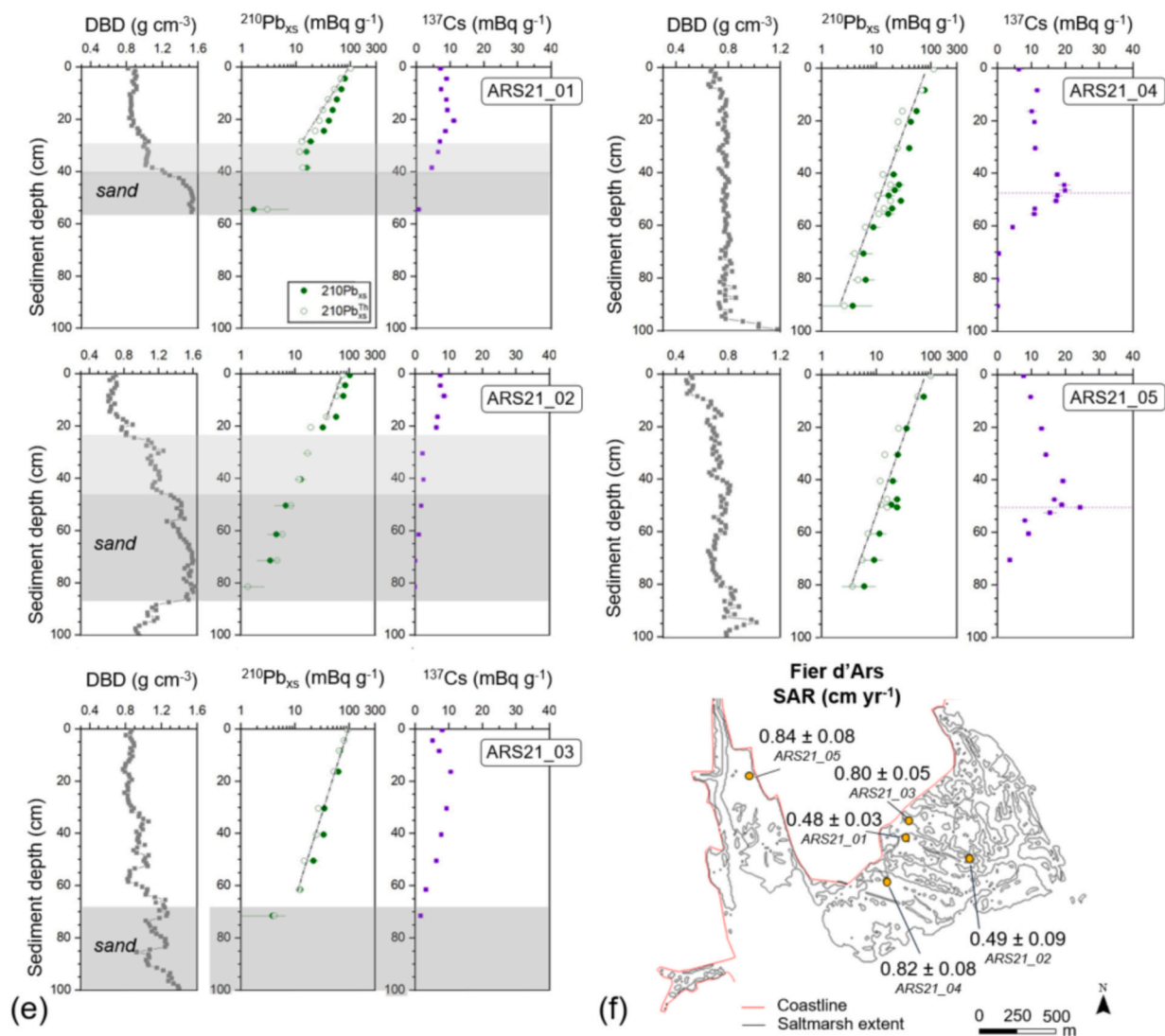


Fig. 3. (continued).

Consequently, the lateral expansion of saltmarsh vegetation is strongly influenced by the inherited geomorphology, such as a bay's orientation towards prevailing winds (e.g., Fier d'Ars) and the presence of natural protective features (e.g., sand spits in Aiguillon). These protective features and sheltered bay heads facilitate faster lateral progradation, emphasizing the importance of natural coastal geomorphologies in controlling saltmarsh evolution.

The sediment availability in the coastal waters of the Pertuis Charentais Sea creates favorable conditions that contribute to the overall progradation of the studied saltmarshes (Ge et al., 2015; Fagherazzi et al., 2020). However, while high sediment availability likely explains the general trend of saltmarsh progradation, coastal SSC did not emerge as a significant factor in accounting for the observed spatial variability in the lateral evolution between the studied sites. This contrasts with studies in areas with low fluvial suspended sediment supply, where coastal SSC primarily influences the lateral expansion and erosion of saltmarshes (Ladd et al., 2019).

The overall vegetation progradation observed in all the saltmarshes of the Pertuis Charentais underlines their ability to adapt and expand in response to changing environmental conditions. Variations in the rate of vegetation development suggest potential differences in hydrodynamic conditions and degree of exposure to wind and waves, themselves influenced by site-specific geomorphology. Understanding these factors is crucial for effective coastal management and conservation efforts, as

they determine the resilience and adaptability of saltmarsh ecosystems to environmental change, particularly in the context of climate change and sea-level rise.

5.2. Controls on sediment accumulation rates

5.2.1. Inundation frequency and accommodation space

Results revealed an upward trend in sediment accumulation rates along the cross-shore transects, progressing from landward to seaward locations as observed in Aiguillon and Brouage. This could not be inferred in Fier d'Ars as the coring campaign did not follow the same cross-shore strategy. This landward-seaward pattern is consistent with previous studies that highlighted the role of prolonged and frequent inundation of seaward saltmarshes in enhancing sediment supply and deposition (D'Alpaos et al., 2011; Fagherazzi et al., 2020; Fagherazzi et al., 2012). Sediment accretion rates and vertical growth of saltmarshes tend to decrease exponentially with distance from the marsh edge, channels and creeks (D'Alpaos et al., 2007; Zhang et al., 2019). In particular, saltmarsh vegetation can enhance deposition rates so that the amount of sediment available in suspension decreases rapidly away from the saltmarsh seaward margin. As a consequence, the banks of tidal creeks tend to accrete faster than the inner area of the marsh (Townend et al., 2011).

Under high sediment supply, low-elevation saltmarshes can rapidly

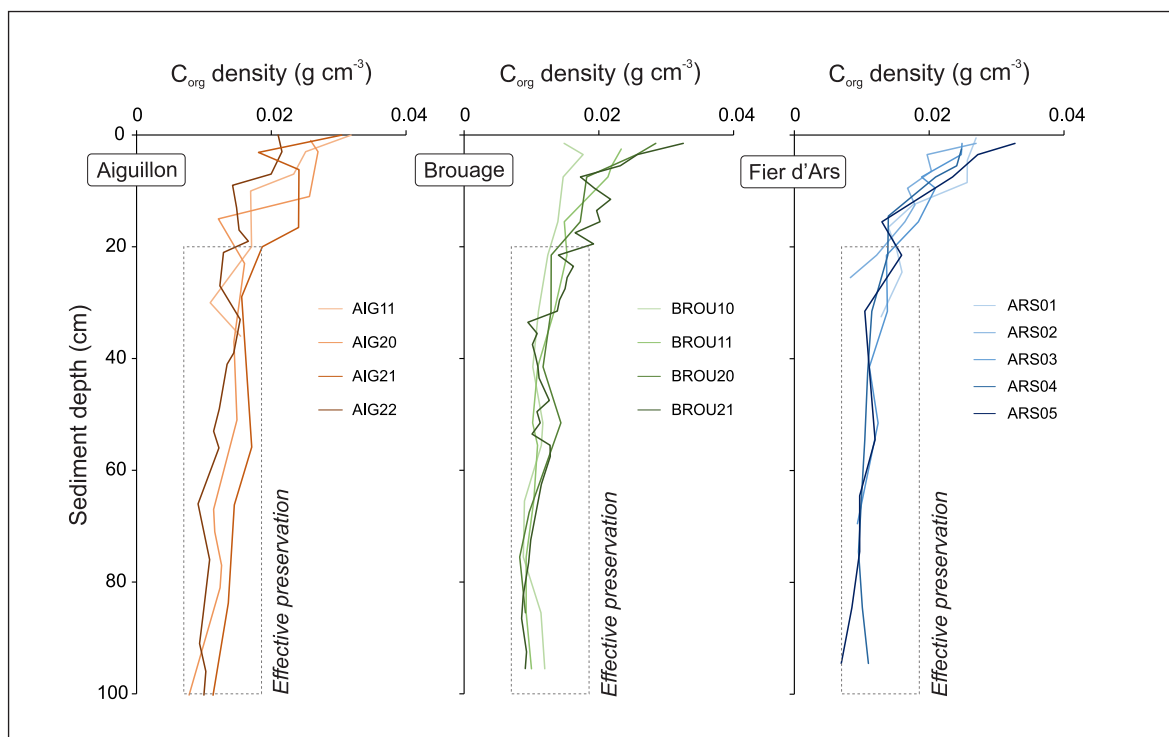


Fig. 4. Comparison of the C_{org} density profiles in the different cores of Aiguillon, Brouage and Fier d'Ars. The downcore stability in these profiles are used as indication for effective preservation of organic carbon content in the sediment cores.

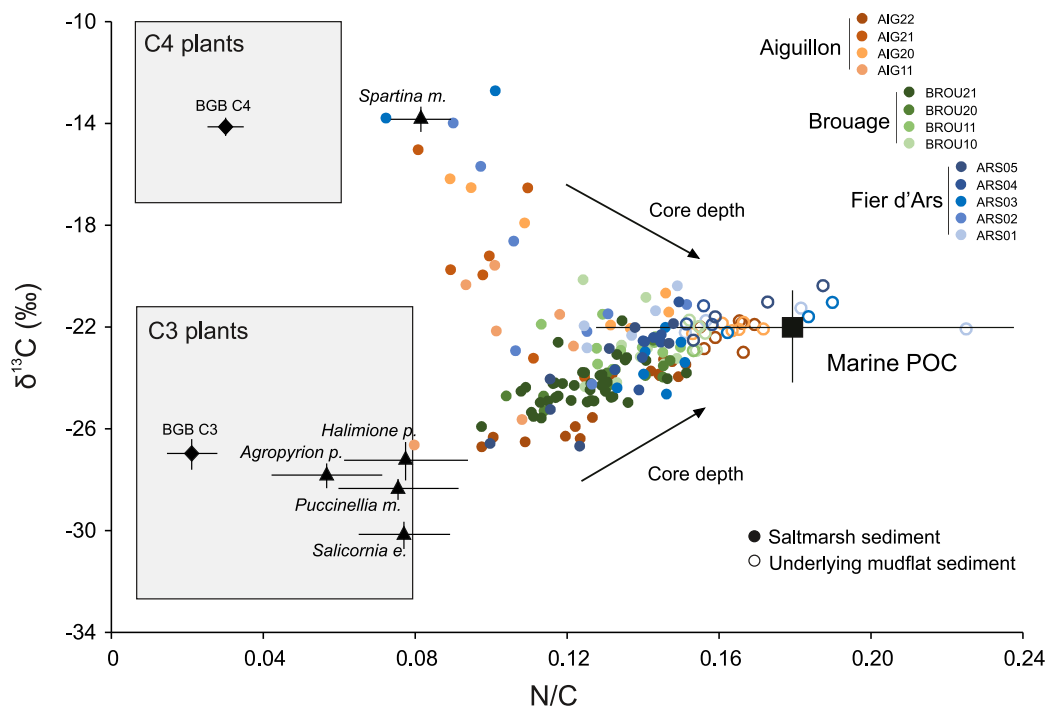


Fig. 5. Comparison of $\delta^{13}C$ and N/C signatures of saltmarsh sediments from Aiguillon (orange circles), Brouage (green circles) and Fier d'Ars (blue circles) in relation to C_{org} sources. Sediments are categorized based on deposition within the cores, distinguishing saltmarsh sediments (solid circles) from underlying mudflat sediments (open circles). C_{org} sources include allochthonous marine particulate organic carbon (marine POC; black square; SOMLIT data), and C_{org} derived from saltmarsh vegetation. The signature of saltmarsh plants (black triangles; this study) and below ground biomass (BGB black diamonds; this study) are compared with the saltmarsh C3- and C4-plant signature from the literature (gray areas; Lamb et al., 2006 and references therein).

expand to an equilibrium elevation relative to the highest water level, while higher elevation saltmarshes tend to maintain this equilibrium (Temmerman et al., 2004; Unger et al., 2016). This process is intrinsic to

the accommodation space between the marsh upper surface and the highest tide levels, which can largely drive sediment and carbon accumulation rates (Schuerch et al., 2018; Rogers et al., 2019). The cross-

Table 2
 $\delta^{13}\text{C}$ (in ‰) and C/N ratio for saltmarsh vegetation and below-ground biomass.

Vegetation type	$\delta^{13}\text{C}$ (‰)	$\delta^{13}\text{C}_{\text{dev}}$ (‰)	C/N	C/N _{dev}
<i>Spartina maritima</i>	-13.91	0.49	12.35	1.32
<i>Puccinellia maritima</i>	-28.42	0.38	13.73	2.91
<i>Salicornia europea</i>	-30.21	0.52	13.24	2.10
<i>Agropyron pungentis</i>	-27.87	0.48	18.94	5.83
<i>Halimione portulacoides</i>	-27.28	0.72	13.40	2.80
BGB_C4	-14.18	0.29	33.98	5.95
BGB_C3	-27.02	0.59	50.40	15.23

shore pattern observed in the studied saltmarshes was also spatially corroborated at the decadal scale using LiDAR mapping in Aiguillon Bay (Amann et al., 2023). Taken together, these observations suggest that the intra-site SAR gradient could be attributed to variations in inundation frequency (and accommodation space), and to distance from sediment sources provided by mudflats and tidal channels.

Transitioning from examining sediment accumulation rates within individual sites to understanding variability between sites, the unique case of Fier d'Ars emerges. Despite experiencing more frequent inundation and having greater accommodation space, Fier d'Ars exhibits lower sediment accumulation rates than expected. As a result, no significant correlation was found between inundation frequency and SAR at the coring locations among the three sites. Since inundation frequency and accommodation space do not by themselves explain the observed

variation, additional variables such as sediment availability must be considered to explain the inter-site variability.

5.2.2. Sediment availability

The variation in sediment accumulation rates among the studied sites highlights the importance of sediment availability in shaping vertical accretion processes. Specifically, the SAR in the Fier d'Ars ($0.69 \pm 0.18 \text{ cm yr}^{-1}$) is notably lower than that in Aiguillon and Brouage ($1.51 \pm 0.54 \text{ cm yr}^{-1}$ and $1.64 \pm 0.36 \text{ cm yr}^{-1}$, respectively). This difference is closely related to variations in the suspended sediment concentration (SSC) of the coastal water. SSC is lower in front of the Fier d'Ars ($7.5 \pm 3.3 \text{ g m}^{-3}$) compared to Aiguillon and Brouage ($23.7 \pm 6.8 \text{ g m}^{-3}$ and $29.8 \pm 5.8 \text{ g m}^{-3}$, respectively). The offshore location of the Fier d'Ars, far from riverine sediment sources, probably contributes to this reduced sediment availability. Additionally, the orientation of the embayment of the Fier d'Ars with the respect to the prevailing wind directions (WSW to WNW) is likely to exacerbate this limitation, further hindering sediment remobilization by wind waves and subsequent deposition.

Despite the contrasting geomorphologies, both Aiguillon and Brouage exhibit high SAR values. This suggests that sediment availability, rather than protection from wind and waves, is likely to play a more important role in determining patterns of vertical accretion rates in these coastal ecosystems. Coastal suspended sediment concentration and saltmarsh sediment accretion are strongly linked (Allen, 2000; D'Alpaos et al., 2007; Fagherazzi et al., 2020), with factors that increase SSC can

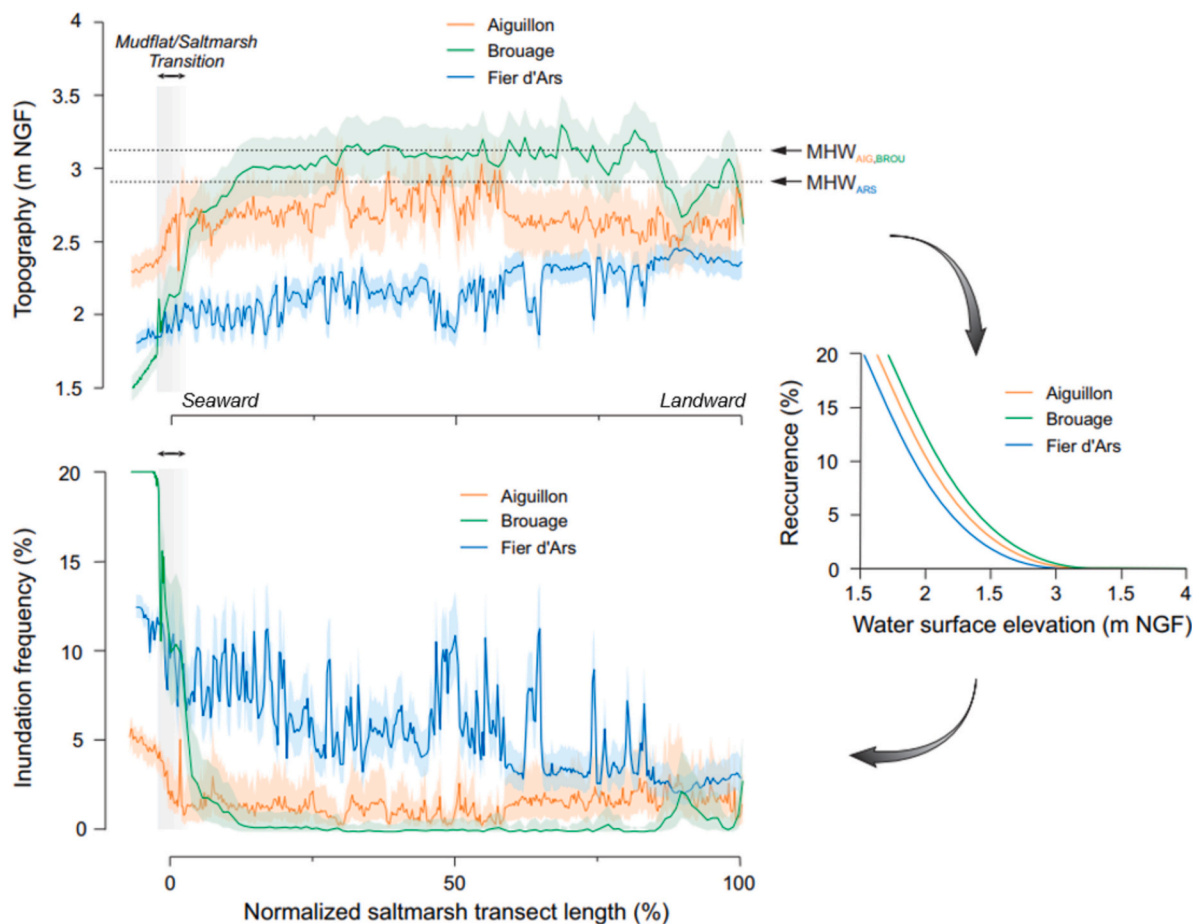


Fig. 6. Intertidal topography and inundation frequency of for the three sites, with (*upper*) averaged topographic profile of cross-shore transects, and (*lower panel*) inundation frequency calculated using topographical profiles and water elevation recurrence curves specific to each site (*right panel*). The distance of the saltmarsh transects on the x-axis was normalized as a percentage (%) to allow graphical comparison between sites (100 % refers to the maximum distance between the saltmarsh boundary and the dike, specific to each study site). Mean high water values (hereafter referred to as MHW) are related to water surface elevation with a 0.01 % recurrence. Topography is based on LiDAR-derived DEMs; credits: © CD17 – MNT – 2021 for Brouage and Fier d'Ars, © OPSIA Company, LIFE Program Aiguillon Bay 2016–2022 for Aiguillon.

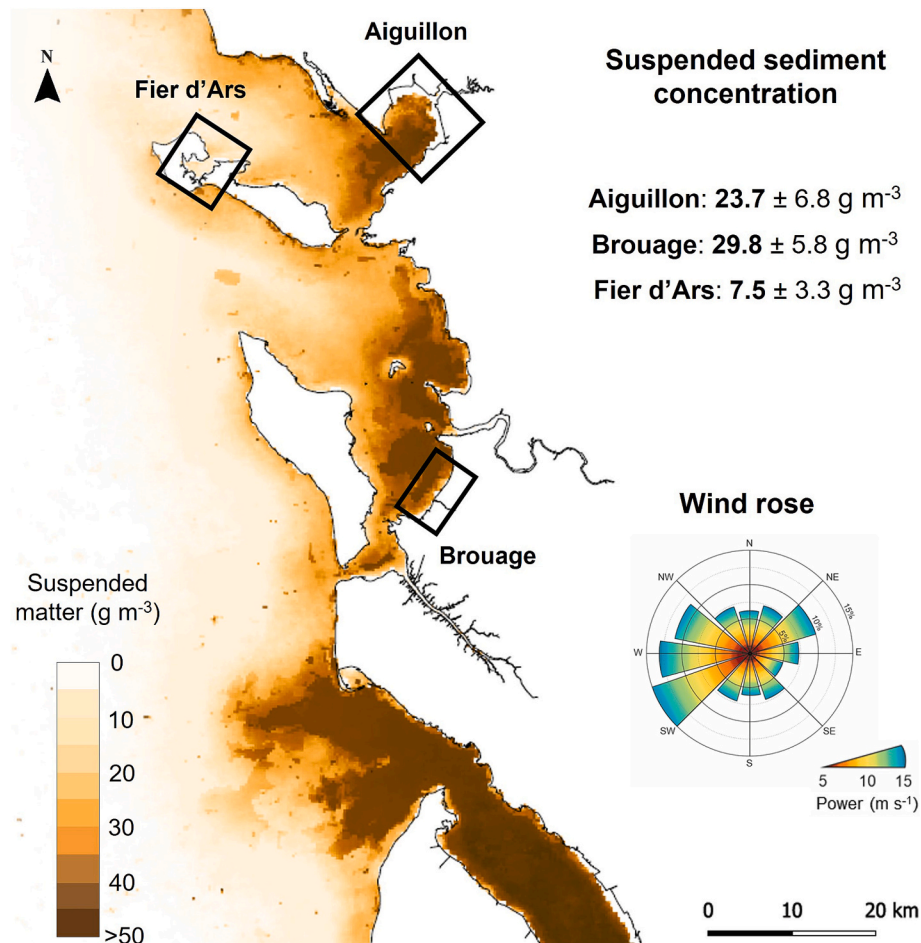


Fig. 7. Mapping of annual mean coastal suspended particulate matter concentration (in g m^{-3}) for the period 2016–2021, and associated averages for the three study sites. Data refer to inorganic suspended particulate matter derived from ocean colour (SPM-R, Aqua MODIS; [Novoa et al., 2017](#)). The wind rose was generated through the global wind atlas interface using the ERA5 dataset for the period 2008–2017 ([www.globalwindatlas.info](#)).

also enhancing the minerogenic contribution to saltmarsh accretion ([Friedrichs, 2011](#); [Friedrichs and Perry, 2001](#)). High turbidity in coastal waters of the region, caused primarily by the resuspension of muddy sediments with each tide, is exacerbated by strong wind waves and floods ([Bassoullet et al., 2000](#); [Poirier et al., 2010, 2016](#)). Wind waves can re-suspend river-fed sediments and distribute them across the marsh platform, eventually allowing for vertical accretion. The extensive intertidal mudflats in the Pertuis Charentais Sea contribute significantly to this phenomenon by facilitating the transport of fine sediment between the lower and upper mudflats and towards the saltmarsh platforms ([Bassoullet et al., 2000](#); [Le Hir et al., 2010](#); [Poirier et al., 2010](#)). This emphasizes the critical role of sediment dynamics, particularly suspended sediment concentration, in shaping the vertical evolution of minerogenic saltmarshes.

5.3. Implications for carbon burial and sequestration

The mean carbon burial rate for the three sites of the Pertuis Charentais Sea is $231 \pm 58 \text{ gC m}^{-2} \text{ yr}^{-1}$ ([Table 1](#)), aligning closely with the global average for saltmarshes of $245 \pm 26 \text{ gC m}^{-2} \text{ yr}^{-1}$ ([Ouyang and Lee, 2014](#); [Regnier et al., 2022](#)). Results from this study provide valuable site-specific data to improve blue carbon review efforts ([Chmura et al., 2003](#); [Duarte et al., 2005](#); [Murray et al., 2011](#); [McLeod et al., 2011](#); [Ouyang and Lee, 2014](#); [Regnier et al., 2022](#)). To date, only one French study focusing on Mediterranean estuarine saltmarshes has contributed to these efforts ([Hensel et al., 1999](#)), emphasizing the importance of this work. Although European saltmarshes represent only 7.3 % of the global

saltmarsh surface area ([Rosentreter et al., 2023](#)), they prove a resilient capacity to cope with sea level rise and act as significant carbon sinks (e.g., [Mazarrasa et al., 2023](#); [Rosentreter et al., 2023](#)). Our observations from saltmarshes in southwest France further support this resilience and carbon sink capacity.

Results also highlighted an important spatial variability in C_{org} burial rates, which is strongly correlated with sediment accumulation rates. This relationship holds across the Pertuis Charentais region, confirming the key role of sediment accumulation rates in subsurface C_{org} stocks and burial rates in minerogenic marshes ([Amann et al., 2023](#); [Martinetto et al., 2023](#); [Van de Broek et al., 2018](#)). The relationship between SAR and C_{org} burial rates has important implications for upscaling C_{org} sequestration rates from minerogenic saltmarshes, and highlights the importance of considering morphological studies of saltmarshes in understanding the carbon sink function of these ecosystems. Previous works have highlighted the substantial global variation in C_{org} burial rates from coastal wetlands ranging from 10- to 600-fold ([Duarte, 2017](#); [Williamson and Gattuso, 2022](#)). Results for saltmarshes from the Pertuis Charentais Sea revealed a fivefold range at the level of individual sites and within a climatically uniform region (75 to $345 \text{ gC m}^{-2} \text{ yr}^{-1}$). This highlights the importance of conducting multiple coring campaigns to accurately estimate C_{org} burial in saltmarshes.

The isotopic signatures of carbon ($\delta^{13}\text{C}$) and nitrogen-carbon ratios (N/C) in saltmarsh sediments further support previous research indicating the prevalence of allochthonous marine carbon in long-term C_{org} accumulation in minerogenic saltmarshes ([Van de Broek et al., 2018](#)). Data suggest that a marine source dominates the C_{org} signature of

downcore sediment samples, with basal-core samples corresponding to mudflat sediments ($\delta^{13}\text{C} = -22.0 \pm 0.2 \text{ ‰}$; $\text{N/C} = 0.15 \pm 0.01$). This observed pattern was discussed in great detail for the Aiguillon Bay by Amann et al. (2023), and is confirmed here for Brouage and Fier d'Ars (Fig. 4). While the surface organic carbon pools are mainly of autochthonous origin, only a fraction persists with sediment depth and contributes to long-term carbon sequestration rates. This suggests that these ecosystems act as effective traps for allochthonous C_{org} , promoting the importance of considering coupled mudflat-marsh systems in blue carbon coastal ecosystem assessments (Macreadie et al., 2019).

Saltmarsh ecosystems, particularly in the Pertuis Charentais Sea, act as important carbon sinks by trapping, accumulating, and isolating organic carbon from the environment. These ecosystems have the capacity to sequester up to 8.4 TCO_2eq per hectare annually. To contextualize, a single hectare of saltmarsh can offset the annual carbon footprint of an average French citizen, which stands at 8.2 TCO_2eq (DATA-LAB France, 2022). This remarkable carbon sequestration potential aligns with the urban community of La Rochelle's carbon neutrality ambitions, as outlined in the La Rochelle Zero Net Carbon Territory (LRTZC) project. The saltmarshes of the Pertuis Charentais Sea are proving to be invaluable assets in supporting the city's goal of achieving carbon neutrality by 2040 (<https://www.larochelle-zero-carbone.fr/notre-defi>).

While the significant carbon sequestration potential of these saltmarshes is evident, it is important to recognize that the overall effectiveness of long-term carbon storage can be influenced by the proportion of labile (easily degradable) versus non-labile (more stable) organic carbon. Although this study focuses specifically on carbon accumulation rates and does not assess the lability of the stored carbon, understanding these proportions would provide a more nuanced view of the long-term sequestration. Incorporating such an analysis in future research could further enhance the assessment of saltmarshes' role in long-term carbon storage and climate mitigation.

5.4. Implications for coastal marsh management

Effective coastal marsh management necessitates a holistic approach that integrates all natural processes with strategic interventions. By prioritizing the preservation of accommodation space, sediment continuity, and leveraging natural progradation, coastal managers can enhance the resilience of saltmarsh ecosystems and maximize their socio-economic and environmental benefits.

5.4.1. Strategic utilization of saltmarshes for coastal resilience

Integrating the natural processes of progradation and accretion into coastal planning and decision-making can significantly enhance the resilience and functionality of coastal ecosystems. This strategic approach includes allowing natural progradation, realigning coastal infrastructure to accommodate these processes, and restoring coastal ecosystems to promote saltmarsh expansion and sediment deposition. For example, increasing the vegetated shoreline area and promoting sediment deposition can be achieved through the installation of living shorelines, such as coir logs and bags of oyster shell (Wigand et al., 2017). These measures aim to protect coastlines and enhance ecosystem services, as recognized by the UNFCCC (2021).

5.4.2. Role of accommodation space and sediment supply

Accommodation space and sediment supply are key in sustaining saltmarshes in the Pertuis Charentais Sea amidst changing coastal dynamics. Review studies have projected a significant loss of global coastal wetland area, ranging from 20 to 90 % by 2100, attributed to sea-level rise (for low- and high SLR scenarios, respectively; Spencer et al., 2016). However, by accounting for vertical accretion through sediment deposition and lateral expansion via colonizing vegetation, projected global losses can be reduced to between 0 and 30 % (Schuerch et al., 2018). Maintaining adequate accommodation space and sediment supply is

essential for the continued lateral and vertical progression of coastal marshes. A non-interventionist approach, such as 'laissez-faire' management, can be effective for naturally prograding and vertically accreting saltmarshes that outpace sea-level rise. (e.g., Aiguillon). In contrast, saltmarsh systems with limited morphological evolution (e.g., Brouage) rely solely on managed realignment to create additional accommodation space, enabling inland migration of saltmarsh plant species and thereby enhancing saltmarsh resilience and ecosystem service provision.

5.4.3. Leveraging progradation and accretion

The saltmarshes in the Pertuis Charentais Sea have demonstrated rapid rates of progradation and accretion, presenting opportunities for strategic realignment initiatives to capitalize on coastal wetlands' ecosystem services. These services are particularly significant in terms of their carbon sink function, with some of the highest global carbon burial capacities recorded. A relevant regional demonstration of this can be seen in Mortagne-sur-Gironde (Gironde Estuary), where a storm in 1999 breached dikes, leaving the site connected to the sea and triggering rapid sediment deposition and natural filling (up to 7.5 cm yr^{-1} for the period 2001–2021; Dupere, 2021). This example highlights the potential effectiveness of managed realignment strategies in the region, leveraging fast accumulation rates and halophytic vegetation development to drive efficient landscape changes and enhance ecosystem services.

5.4.4. Ensuring sediment continuity

Results from this study point out the critical role of sediment availability in maintaining the physical health of saltmarsh ecosystems. Ensuring continuous sediment supply in coastal rivers is imperative to optimize ecosystem services and to support managed realignment strategies. This involves preventing sediment loss from anthropogenic activities and promoting sediment transport processes essential for marsh sustainability. Dams, in particular, disrupt natural sediment flow, increasing the vulnerability of nearby saltmarshes to erosion and habitat loss (Syvitski et al., 2022). The Ebro Delta in Spain serves as a striking example in Europe, where 99 % of sediment is retained by extensive damming, resulting in accelerated degradation of the coastal saltmarsh ecosystems (Rodríguez-Santalla and Somoza, 2019). This demonstrated the negative impact of dams on saltmarsh ecosystems, also emphasizing the importance of addressing sediment deficits to mitigate erosion and maintain ecosystem health.

6. Conclusion

This study investigated the factors influencing the morphological dynamics and carbon accumulation in macrotidal minerogenic saltmarshes within the Pertuis Charentais region in France, focusing on key coastal factors shaping these ecosystems.

Wind-wave exposure itself controlled by coastal geomorphologies emerged as a critical factor that shapes lateral saltmarsh growth, with protected areas generally exhibiting faster progradation rates compared to more exposed locations prone to erosion. Suspended sediment concentrations (SSC) in coastal waters were found to play a central role in governing between-site variability in sediment accretion rates. Sites with higher SSC typically experience greater sediment accumulation, highlighting the importance of sediment availability in fostering saltmarsh resilience.

Carbon burial rates closely correlate with sediment dynamics, emphasizing the importance of sediment availability in carbon sequestration capacity by minerogenic saltmarshes. Isotopic analyses confirm the significant contribution of marine-derived carbon to long-term carbon accumulation processes within these ecosystems. This supports prior research indicating that carbon accumulation rates in these ecosystems depend not only on marsh morphology, and vegetation's carbon burial capacity, but also on the broader coastal ecosystem, including

nearshore waters and mudflat productivity. Viewing saltmarshes as part of a coupled mudflat-marsh system is essential for understanding carbon dynamics and sequestration rates.

Effective coastal management strategies should prioritize ensuring continuous sediment supply in coastal rivers, preserving and allowing accommodation space, and leveraging natural progradation to enhance saltmarsh resilience. Bridging gaps in our understanding of these ecosystems also supports global efforts in blue carbon sequestration and promotes the sustainable use of coastal resources. This integrated approach strengthens the resilience of coastal ecosystems, ensuring their continued benefits for both human societies and the environment.

CRedit authorship contribution statement

Amann Benjamin: Writing – original draft, Visualization, Validation, Methodology, Investigation, Funding acquisition, Formal analysis, Data curation, Conceptualization. **Chaumillon Eric:** Writing – review & editing, Validation, Supervision, Investigation, Funding acquisition, Conceptualization. **Bertin Xavier:** Writing – review & editing, Investigation, Data curation. **Pignon-Mussaud Cécilia:** Writing – review & editing, Visualization, Investigation. **Marie-Claire Perello:** Writing – review & editing, Formal analysis, Data curation. **Christine Dupuy:** Writing – review & editing, Project administration, Funding acquisition, Conceptualization. **Long Nathalie:** Writing – review & editing, Project administration, Funding acquisition. **Schmidt Sabine:** Writing – review & editing, Investigation, Formal analysis, Data curation, Conceptualization.

Declaration of competing interest

The authors declare that they have no known competing financial interests or personal relationships that could have appeared to influence the work reported in this paper.

Acknowledgments

This research was supported by the *PAMPAS* project (ANR-18-32CE-0006-01), and the project *La Rochelle Territoire Zero Carbone* (LRTZC, Carbon Bleu Axe2 OPE-2021-0376, OPE-2021-0496). This work is also part of the *Carbonium* project within the Priority Research Programmes and Equipments (PEPR) “FairCarboN”, which received national funding under the label France 2030 initiative (ANR-22-PEXF-006). We would like to thank Jean-Christophe Lemesle (Conservator RNN Lilleau des Niges, Fier d’Ars), Régis Gallais (OFB) and Jean-Pierre Guéret (LPO, Conservators RNN Aiguillon Bay), and Pamela Lagrange (LPO Scientific project manager, Rochefort), for their support in field campaigns, for sharing their expertise, and for granting access in the saltmarsh sites. Particular thanks also go to Laura Olivier and Jasson Mora Mussio (LIENSs, CNRS-La Rochelle University) for their contribution to the reconstruction of the saltmarsh boundary, and to Benoit Othoniel (LIENSs, CNRS-La Rochelle University) for his help and shared knowledge about the role of coastal marshes as support for nature-based solutions. Finally, we want to thank Bénédicte Dubillot for her enthusiasm and support with the carbon isotope data, and Gaël Guillou and Benoit Lebreton (LIENSs, CNRS-La Rochelle University) for their support with the IRMS platform.

Data availability

Data will be made available on request.

References

Allen, J., 2000. Morphodynamics of Holocene salt marshes: a review sketch from the Atlantic and Southern North Sea coasts of Europe. *Quat. Sci. Rev.* 19, 1155–1231. [https://doi.org/10.1016/S0277-3791\(99\)00034-7](https://doi.org/10.1016/S0277-3791(99)00034-7).

- Amann, B., Chaumillon, E., Schmidt, S., Olivier, L., Jupin, J., Perello, M.C., Walsh, J.P., 2023. Multi-annual and multi-decadal evolution of sediment accretion in a saltmarsh of the French Atlantic coast: Implications for carbon sequestration. *Estuarine, Coastal and Shelf Science* 293, 108467. <https://doi.org/10.1016/j.ecss.2023.108467>.
- Baranes, H.E., Woodruff, J.D., Geyer, W.R., Yellen, B.C., Richardson, J.B., and Griswold, F., 2022. Sources, Mechanisms, and Timescales of Sediment Delivery to a New England Salt Marsh: *Journal of Geophysical Research: Earth Surface*, v. 127, p. e2021JF006478, <https://doi.org/10.1029/2021JF006478>.
- Bassoullet, Ph., Le Hir, P., Gouleau, D., Robert, S., 2000. *Sediment Transport over an Intertidal Mudflat: Field Investigations and Estimation of Fluxes within the “Baie de Marennes-Oleron”*, vol. v. 20. *Continental Shelf Research, France*, pp. 1635–1653.
- Bertin, X., Bruneau, N., Breilh, J.-F., Fortunato, A.B., Karpytchev, M., 2012. Importance of wave age and resonance in storm surges: the case Xynthia. *Bay of Biscay: Ocean Modelling* 42, 16–30. <https://doi.org/10.1016/j.ocemod.2011.11.001>.
- Bertin, X., Li, K., Roland, A., Bidlot, J.-R., 2015. The contribution of short-waves in storm surges: two case studies in the Bay of Biscay. *Cont. Shelf Res.* 96, 1–15. <https://doi.org/10.1016/j.csr.2015.01.005>.
- Bertram, C., Quaas, M., Reusch, T.B.H., Vafeidis, A.T., Wolff, C., Rickels, W., 2021. The blue carbon wealth of nations: *Nature. Climate Change* 11, 704–709. <https://doi.org/10.1038/s41558-021-01089-4>.
- Bij de Vaate, I., Brückner, M.Z.M., Kleinhans, M.G., Schwarz, C., 2020. On the Impact of Salt Marsh Pioneer Species-Assemblages on the Emergence of Intertidal Channel Networks. *Water Resour. Res.* 56. <https://doi.org/10.1029/2019WR025942>.
- Bocher, P., Piersma, T., Dekinga, A., Kraan, C., Yates, M.G., Guyot, T., Folmer, E.O., Radenac, G., 2007. Site- and species-specific distribution patterns of molluscs at five intertidal soft-sediment areas in Northwest Europe during a single winter. *Mar. Biol.* 151, 577–594. <https://doi.org/10.1007/s00227-006-0500-4>.
- Bongarts Lebbe, T., et al., 2021. Designing Coastal Adaptation strategies to Tackle Sea Level rise: *Frontiers in Marine. Science* 8, 740602. <https://doi.org/10.3389/fmars.2021.740602>.
- Chmura, G.L., Anisfeld, S.C., Cahoon, D.R., Lynch, J.C., 2003. Global carbon sequestration in tidal, saline wetland soils. *Glob. Biogeochem. Cycles* 17. <https://doi.org/10.1029/2002GB001917> p. n/a-n/a.
- Constantin, S., Doxaran, D., Derkacheva, A., Novoa, S., Lavigne, H., 2018. Multi-temporal dynamics of suspended particulate matter in a macro-tidal river Plume (the Gironde) as observed by satellite data: *Estuarine, Coastal and Shelf Science* 202, 172–184. <https://doi.org/10.1016/j.ecss.2018.01.004>.
- D’Alpaos, A., Lanzoni, S., Marani, M., Rinaldo, A., 2007. Landscape evolution in tidal embayments: Modeling the interplay of erosion, sedimentation, and vegetation dynamics. *J. Geophys. Res.* 112, F01008. <https://doi.org/10.1029/2006JF000537>.
- D’Alpaos, A., Mudd, S.M., Carniello, L., 2011. Dynamic response of marshes to perturbations in suspended sediment concentrations and rates of relative sea level rise. *J. Geophys. Res.* 116, F04020. <https://doi.org/10.1029/2011JF002093>.
- DATA-LAB France, 2022. Chiffres clés du climat France, Europe et Monde: v. www.statistiques.developpement-durable.gouv.fr, p. 92pp.
- Degré, D., et al., 2006. Comparative analysis of the food webs of two intertidal mudflats during two seasons using inverse modelling: Aiguillon Cove and Brouage Mudflat, France: *Estuarine, Coastal and Shelf Science* 69, 107–124. <https://doi.org/10.1016/j.ecss.2006.04.001>.
- Dodet, G., Bertin, X., Bouchette, F., Gravelle, M., Testut, L., Wöppelmann, G., 2019. Characterization of Sea-level Variations along the Metropolitan Coasts of France: Waves, Tides, Storm Surges and Long-term Changes: *Journal of Coastal Research* 88, 10. <https://doi.org/10.2112/S188-003.1>.
- Doxaran, D., Froidefond, J.-M., Castaing, P., Babin, M., 2009. Dynamics of the turbidity maximum zone in a macrotidal estuary (the Gironde, France): Observations from field and MODIS satellite data: *Estuarine, Coastal and Shelf Science* 81, 321–332. <https://doi.org/10.1016/j.ecss.2008.11.013>.
- Duarte, C.M., 2017. Reviews and syntheses: Hidden forests, the role of vegetated coastal habitats in the ocean carbon budget: *Biogeosciences*, v. 14, p. 301–310, doi:<https://doi.org/10.5194/bg-14-301-2017>.
- Duarte, C.M., Middelburg, J.J., and Caraco, N., 2005. Major role of marine vegetation on the oceanic carbon cycle: p. 8.
- Dupere, 2021. Etude sédimentaire sur l’ancien polder aval de Mortagne-sur-Gironde, *Compte-rendu d’étude commandée par le Conservatoire de l’espace littoral et des rivages lacustres*, 23 pages, Eco Metrum.
- Esteves, L.S., 2014. *Managed Realignment : a Viable Long-Term Coastal Management Strategy?* Dordrecht, Springer Netherlands, SpringerBriefs in Environmental Science, doi:<https://doi.org/10.1007/978-94-017-9029-1>.
- Fagherazzi, S., Mariotti, G., Leonardi, N., Canestrelli, A., Nardin, W., Kearney, W.S., 2020. Salt Marsh Dynamics in a period of Accelerated Sea Level Rise. *J. Geophys. Res.* Earth 125. <https://doi.org/10.1029/2019JF005200>.
- Fagherazzi, S., Torres, R., Hopkinson, C., Van Proosdij, D., 2005. Salt marsh geomorphology: Physical and ecological effects on landform: *Eos. Trans. Am. Geophys. Union* 86, 57. <https://doi.org/10.1029/2005EO060002>.
- Fagherazzi, S., et al., 2012. Numerical models of salt marsh evolution: Ecological, geomorphic, and climatic factors. *Rev. Geophys.* 50. <https://doi.org/10.1029/2011RG000359> p. RG1002.
- Finotello, A., Marani, M., Carniello, L., Pivato, M., Roner, M., Tommasini, L., D’Alpaos, A., 2020. Control of wind-wave power on morphological shape of salt marsh margins. *Water Science and Engineering* 13, 45–56. <https://doi.org/10.1016/j.wse.2020.03.006>.
- Friedrichs, C.T., 2011. Tidal Flat Morphodynamics, in *Treatise on Estuarine and Coastal Science*, Elsevier, p. 137–170, doi:<https://doi.org/10.1016/B978-0-12-374711-2.00307-7>.

- Friedrichs, C.T., Perry, J.E., 2001. Tidal Salt Marsh Morphodynamics: a Synthesis. *J. Coast. Res.* 27, 32.
- Ge, Z.-M., Zhang, L.-Q., Yuan, L., 2015. Spatiotemporal Dynamics of Salt Marsh Vegetation regulated by Plant Invasion and Abiotic Processes in the Yangtze Estuary: Observations with a Modeling Approach. *Estuar. Coasts* 38, 310–324. <https://doi.org/10.1007/s12237-014-9804-7>.
- Griggs, G., Reguero, B.G., 2021. Coastal Adaptation to climate Change and Sea-Level rise. *Water* 13, 2151. <https://doi.org/10.3390/w13162151>.
- Hensel, P.F., Day Jr., J.W., Pont, D., 1999. Wetland Vertical Accretion and Soil Elevation Change in the Rhone River Delta, France: The Importance of Riverine Flooding v. 15, 668–681.
- Himmelstoss, E.A., Henderson, R.E., Kratzmann, M.G., and Farris, A.S., 2018, Digital Shoreline Analysis System DSAS Version 5.0 User Guide." Open-File Report 2018-1179: 126.: v. Open-File Report 1179, p. 126.
- Huguet, J.-R., Bertin, X., Arnaud, G., 2018. Managed realignment to mitigate storm-induced flooding: a case study in La Faute-sur-mer, France. *Coast. Eng.* 134, 168–176. <https://doi.org/10.1016/j.coastaleng.2017.08.010>.
- IPCC, 2022. *Climate Change 2022: Mitigation of climate Change*. Skea et al., Working Group III contribution to the Sixth Assessment Report of the Intergovernmental Panel on climate Change. Summary for Policymakers 99.
- Kirwan, M.L., Guntenspergen, G.R., 2010. Influence of tidal range on the stability of coastal marshland: TIDAL RANGE AND MARSH STABILITY. *J. Geophys. Res. Earth* 115. <https://doi.org/10.1029/2009JF001400>.
- Kirwan, M.L., Mudd, S.M., 2012. Response of salt-marsh carbon accumulation to climate change. *Nature* 489, 550–553. <https://doi.org/10.1038/nature11440>.
- Koppel, J. van de, Wal, D. van der, Bakker, J.P., Herman, P.M.J., 2005. Self-Organization and Vegetation Collapse in Salt Marsh Ecosystems. *Am. Nat.* 165, E1–E12. <https://doi.org/10.1086/426602>.
- Ladd, C.J.T., Duggan-Edwards, M.F., Bouma, T.J., Pagès, J.F., Skov, M.W., 2019. Sediment Supply explains Long-Term and Large-Scale patterns in Salt Marsh Lateral expansion and Erosion. *Geophys. Res. Lett.* 46, 11178–11187. <https://doi.org/10.1029/2019GL083315>.
- Lamb, A.L., Wilson, G.P., Leng, M.J., 2006. A review of coastal palaeoclimate and relative sea-level reconstructions using $\delta^{13}C$ and C/N ratios in organic material. *Earth Sci. Rev.* 75, 29–57. <https://doi.org/10.1016/j.earscirev.2005.10.003>.
- Lavaud, L., Lechevalier, A., Coulombier, T., Bertin, X., and Martins, K., 2020. Effet de la végétation sur la dissipation des vagues au niveau d'un pré salé. XVIIIèmes Journées Nationales Génie Côtier – Génie Civil. Le Havre, 2020; doi:<https://doi.org/10.5150/jngcgc.2020.010>.
- Le Hir, P., Kervella, S., Walker, P., Brenon, I., 2010. Erosions, dépôts et transits sédimentaires associés dans le bassin de Marennes-Oléron: La. *Houille Blanche* 96, 65–71. <https://doi.org/10.1051/lhb/2010056>.
- Lebreton, B., Richard, P., Parlier, E.P., Guillou, G., Blanchard, G.F., 2011. Trophic ecology of mullets during their spring migration in a European saltmarsh: a stable isotope study: Estuarine. *Coastal and Shelf Science* 91, 502–510. <https://doi.org/10.1016/j.ecss.2010.12.001>.
- Leonardi, N., Carnacina, I., Donatelli, C., Ganju, N.K., Plater, A.J., Schuerch, M., Temmerman, S., 2018. Dynamic interactions between coastal storms and salt marshes: a review. *Geomorphology* 301, 92–107. <https://doi.org/10.1016/j.geomorph.2017.11.001>.
- Lorrain-Solignon, L., Robin, F., Bertin, X., Jankovic, M., Rousseau, P., Lelong, V., Brischoux, F., 2023. Long-term trends of salinity in coastal wetlands: Effects of climate, extreme weather events, and sea water level. *Environ. Res.* 237, 116937. <https://doi.org/10.1016/j.envres.2023.116937>.
- Macreadie, P.I., et al., 2019. The future of Blue Carbon science: Nature. *Communications* 10, 3998. <https://doi.org/10.1038/s41467-019-11693-w>.
- Mariotti, G., and Fagherazzi, S., 2013. Critical width of tidal flats triggers marsh collapse in the absence of sea-level rise: Proceedings of the National Academy of Sciences, v. 110, p. 5353–5356. <https://doi.org/10.1073/pnas.1219600110>.
- Marani, M., D'Alpaos, A., Lanzoni, S., Santalucia, M., 2011. Understanding and predicting wave erosion of marsh edges. *Geophys. Res. Lett.* 38, L21401. <https://doi.org/10.1029/2011GL048995>.
- Martinetto, P., Alberti, J., Becherucci, M.E., Cebrian, J., Iribarne, O., Marbà, N., Montemayor, D., Sparks, E., Ward, R., 2023. The blue carbon of southern Southwest Atlantic salt marshes and their biotic and abiotic drivers: Nature. *Communications* 14, 8500. <https://doi.org/10.1038/s41467-023-44196-w>.
- Mazarrasa, I., Neto, J.M., Bouma, T.J., Grandjean, T., Garcia-Orellana, J., Masqué, P., Recio, M., Serrano, O., Puente, A., Juanes, J.A., 2023. Drivers of variability in Blue Carbon stocks and burial rates across European estuarine habitats. *Sci. Total Environ.* 886, 163957. <https://doi.org/10.1016/j.scitotenv.2023.163957>.
- McLeod, E., Chmura, G.L., Bouillon, S., Salm, R., Björk, M., Duarte, C.M., Lovelock, C.E., Schlesinger, W.H., Silliman, B.R., 2011. A blueprint for blue carbon: toward an improved understanding of the role of vegetated coastal habitats in sequestering CO₂. *Front. Ecol. Environ.* 9, 552–560. <https://doi.org/10.1890/110004>.
- Mueller, P., Ladiges, N., Jack, A., Schmiel, G., Kutzbach, L., Jensen, K., Nolte, S., 2019. Assessing the long-term carbon-sequestration potential of the semi-natural salt marshes in the European Wadden Sea. *Ecosphere* 10. <https://doi.org/10.1002/ecs2.2556>.
- Murray, B.C., Pendleton, L., Jenkins, W.A., Sifleet, S., 2011. Green Payments for Blue Carbon. *Economic Incentives for Protecting Threatened Coastal Habitats*: V. Nicholas Institute for Environmental Policy, p. 52. Solutions Report NI R 11-04.
- Novoa, S., Doxaran, D., Ody, A., Vanhellemont, Q., Lafon, V., Lubac, B., Gernez, P., 2017. Atmospheric Corrections and Multi-Conditional Algorithm for Multi-Sensor Remote Sensing of Suspended Particulate Matter in Low-to-High Turbidity Levels Coastal Waters. *Remote Sens.* 9, 61. <https://doi.org/10.3390/rs9010061>.
- Ouyang, X., Lee, S.Y., 2013. Carbon accumulation rates in salt marsh sediments suggest high carbon storage capacity. *Biogeochemistry* 10, 1915–19188. <https://doi.org/10.5194/bg-10-1915-2013>.
- Ouyang, X., Lee, S.Y., 2014. Updated estimates of carbon accumulation rates in coastal marsh sediments. *Biogeosciences* 11, 5057–5071. <https://doi.org/10.5194/bg-11-5057-2014>.
- Pétillon, J., et al., 2023. Top ten priorities for global saltmarsh restoration, conservation and ecosystem service research. *Sci. Total Environ.* 898, 165544. <https://doi.org/10.1016/j.scitotenv.2023.165544>.
- Poirier, C., Poitevin, C., Chaumillon, E., 2016. Comparison of estuarine sediment record with modelled rates of sediment supply from a western European catchment since 1500. *Compt. Rendus Geosci.* 348, 479–488. <https://doi.org/10.1016/j.crte.2015.02.009>.
- Poirier, C., Sauriau, P.-G., Chaumillon, E., Bertin, X., 2010. Influence of hydro-sedimentary factors on mollusc death assemblages in a temperate mixed tide-and-wave dominated coastal environment: Implications for the fossil record. *Cont. Shelf Res.* 30, 1876–1890. <https://doi.org/10.1016/j.csr.2010.08.015>.
- Regnier, P., Resplandy, L., Najjar, R.G., Ciais, P., 2022. The land-to-ocean loops of the global carbon cycle. *Nature* 603, 401–410. <https://doi.org/10.1038/s41586-021-04339-9>.
- Rodríguez-Santalla, I., Somoza, L., 2019. The Ebro River Delta. In: Morales, J.A. (Ed.), *The Spanish Coastal Systems*. Springer International Publishing, Cham, pp. 467–488. https://doi.org/10.1007/978-3-319-93169-2_20.
- Rogers, K., et al., 2019. Wetland carbon storage controlled by millennial-scale variation in relative sea-level rise. *Nature* 567, 91–95. <https://doi.org/10.1038/s41586-019-0951-7>.
- Rosentreter, J.A., et al., 2023. Coastal vegetation and estuaries are collectively a greenhouse gas sink: Nature. *Climate Change* 13, 579–587. <https://doi.org/10.1038/s41558-023-01682-9>.
- Rupp-Armstrong, S., Nicholls, R.J., 2007. Coastal and Estuarine Retreat: a Comparison of the Application of managed Realignment in England and Germany. *J. Coast. Res.* 236, 1418–1430. <https://doi.org/10.2112/04-0426.1>.
- Saha, S., et al., 2010. The NCEP climate Forecast System Reanalysis. *Bull. Am. Meteorol. Soc.* 91, 1015–1058. <https://doi.org/10.1175/2010BAMS3001.1>.
- Savelli, R., et al., 2019. Impact of Chronic and massive Resuspension Mechanisms on the Microphytobenthos Dynamics in a Temperate Intertidal Mudflat: Journal of Geophysical Research. *Biogeosciences* 124, 3752–3777. <https://doi.org/10.1029/2019JG005369>.
- Schmidt, S., Amann, B., 2024. Depth profiles of selected radionuclides in marine sediments of three macrotidal saltmarshes of the French Atlantic coast. *SEANOE*. <https://doi.org/10.17882/102639>.
- Schmidt, S., Hova, H., Diallo, A., Martín, J., Cremer, M., Duros, P., Fontanier, C., Deflandre, B., Metzger, E., Mulder, T., 2014. Recent sediment transport and deposition in the Cap-Ferret Canyon, South-East margin of Bay of Biscay. *Deep-Sea Res. II Top. Stud. Oceanogr.* 104, 134–144. <https://doi.org/10.1016/j.dsr2.2013.06.004>.
- Schmitt, A., Chaumillon, E., 2023. Understanding morphological evolution and sediment dynamics at multi-time scales helps balance human activities and protect coastal ecosystems: an example with the Gironde and Pertuis Marine Park. *Sci. Total Environ.* 887, 163819. <https://doi.org/10.1016/j.scitotenv.2023.163819>.
- Schuerch, M., et al., 2018. Future response of global coastal wetlands to sea-level rise. *Nature* 561, 231–234. <https://doi.org/10.1038/s41586-018-0476-5>.
- Spencer, T., Schuerch, M., Nicholls, R.J., Hinkel, J., Lincke, D., Vafeidis, A.T., Reef, R., McFadden, L., Brown, S., 2016. Global coastal wetland change under sea-level rise and related stresses: the DIVA Wetland Change Model. *Glob. Planet. Chang.* 139, 15–30. <https://doi.org/10.1016/j.gloplacha.2015.12.018>.
- Syvitski, J., Ängel, J.R., Saito, Y., Overeem, I., Vörösmarty, C.J., Wang, H., Olago, D., 2022. Earth's sediment cycle during the Anthropocene. *Nature Reviews Earth & Environment* 3, 179–196. <https://doi.org/10.1038/s43017-021-00253-w>.
- Temmerman, S., Govers, G., Wartel, S., Meire, P., 2004. Modelling estuarine variations in tidal marsh sedimentation: response to changing sea level and suspended sediment concentrations. *Mar. Geol.* 212, 1–19. <https://doi.org/10.1016/j.margeo.2004.10.021>.
- Tonelli, M., Fagherazzi, S., Petti, M., 2010. Modeling wave impact on salt marsh boundaries. *J. Geophys. Res. Oceans* 115. <https://doi.org/10.1029/2009JC006026>, p. 2009JC006026.
- Townend, I., Fletcher, C., Knappen, M., Rossington, K., 2011. A review of salt marsh dynamics: a review of salt marsh dynamics. *Water Environ. J.* 25, 477–488. <https://doi.org/10.1111/j.1747-6593.2010.00243.x>.
- Trumper, K., Bertzy, M., Dickson, B., van der Heijden, G., Jenkins, M., Manning, P., 2009. *The Natural Fix? The Role of Ecosystems in Climate Mitigation: A UNEP Rapid Response Assessment*. Cambridge. U.K, United Nations Environment Programme, p. 65.
- UNFCCC, 2021. *Enhancing Resilience of Oceans, Coastal Areas and Ecosystems through Collaborative Partnerships*. Nairobi Work Programme, Bonn.
- Unger, V., Elseiy-Quirk, T., Sommerfield, C., Velinsky, D., 2016. Stability of organic carbon accumulating in *Spartina alterniflora*-dominated salt marshes of the Mid-Atlantic U.S.: Estuarine. *Coastal and Shelf Science* 182, 179–189. <https://doi.org/10.1016/j.ecss.2016.10.001>.
- Van de Broek, M., Vandendriessche, C., Poppelmonde, D., Merckx, R., Temmerman, S., Govers, G., 2018. Long-term organic carbon sequestration in tidal marsh sediments is dominated by old-aged allochthonous inputs in a macrotidal estuary. *Glob. Chang. Biol.* 24, 2498–2512. <https://doi.org/10.1111/gcb.14089>.
- Wang, X., Xin, P., Zhou, Z., Zhang, F., 2023. A systematic review of morphological models of salt marshes. *Water Science and Engineering* 16, 313–323. <https://doi.org/10.1016/j.wse.2023.08.006>.

- Wigand, C., Ardito, T., Chaffee, C., Ferguson, W., Paton, S., Raposa, K., Vandemoer, C., Watson, E., 2017. A climate Change Adaptation Strategy for Management of Coastal Marsh Systems. *Estuar. Coasts* 40, 682–693. <https://doi.org/10.1007/s12237-015-0003-y>.
- Williamson, P., Gattuso, J.-P., 2022. Carbon Removal using Coastal Blue Carbon Ecosystems is Uncertain and Unreliable. With Questionable Climatic Cost-Effectiveness: *Frontiers in Climate* 4, 853666. <https://doi.org/10.3389/fclim.2022.853666>.
- Yando, E.S., et al., 2023. An integrative salt marsh conceptual framework for global comparisons. *Limnology and Oceanography Letters* 8, 830–849. <https://doi.org/10.1002/lol2.10346>.
- Zhang, X., Leonardi, N., Donatelli, C., Fagherazzi, S., 2019. Fate of cohesive sediments in a marsh-dominated estuary. *Adv. Water Resour.* 125, 32–40. <https://doi.org/10.1016/j.advwatres.2019.01.003>.
- Zhang, Y.J., Ye, F., Stanev, E.V., Grashorn, S., 2016. Seamless cross-scale modeling with SCHISM. *Ocean Model* 102, 64–81. <https://doi.org/10.1016/j.ocemod.2016.05.002>.
- Lemesle, et al., 2022. *Plan de gestion 2022–2031 de la Réserve Naturelle Nationale de Lilleau des Niges*. LPO France, p. 560.